

1 **Plant responses to volcanically-elevated CO₂ in two Costa Rican**
2 **forests**

3 Robert R. Bogue^{1,2}, Florian M. Schwandner^{1,3}, Joshua B. Fisher¹, Ryan Pavlick¹, Troy S. Magney¹,
4 Caroline A. Famiglietti¹, Kerry Cawse-Nicholson¹, Vineet Yadav¹, Justin P. Linick¹, Gretchen B.
5 North⁴, Eliecer Duarte⁵

6 ¹Jet Propulsion Laboratory, California Institute of Technology, 4800 Oak Grove Drive, Pasadena, CA 91109, USA

7 ²Geology Department, Occidental College, 1600 Campus Road, Los Angeles, CA 90041, USA

8 ³Joint Institute for Regional Earth System Science and Engineering, University of California Los Angeles, Los
9 Angeles, CA 90095

10 ⁴Biology Department, Occidental College, 1600 Campus Road, Los Angeles, CA 90041, USA

11 ⁵Observatory of Volcanology and Seismology (OVSICORI), Universidad Nacional de Costa Rica, 2386-3000
12 Heredia, Costa Rica

13 Correspondence to: Florian.Schwandner@jpl.caltech.edu

14

15

16

Revised manuscript prepared for:

17

Biogeosciences (Copernicus), <https://www.biogeosciences.net/>

18

REV2 (2018-11-01)

19

20 **Abstract.** We explore the use of active volcanoes to determine the short- and long-term effects of elevated CO₂ on
21 tropical trees. Active volcanoes continuously but variably emit CO₂ through diffuse emissions on their flanks,
22 exposing the overlying ecosystems to elevated levels of atmospheric CO₂. We found tight correlations ($r^2=0.86$ and
23 $r^2=0.74$) between wood stable carbon isotopic composition and co-located volcanogenic CO₂ emissions for two
24 species, which documents the long-term photosynthetic incorporation of isotopically heavy volcanogenic carbon into
25 wood biomass. Measurements of leaf fluorescence and chlorophyll concentration suggest that volcanic CO₂ also has
26 measurable short-term functional impacts on select species of tropical trees. Our findings indicate significant potential
27 for future studies to utilize ecosystems located on active volcanoes as natural experiments to examine the ecological
28 impacts of elevated atmospheric CO₂ in the tropics and elsewhere. Results also point the way toward a possible future
29 utilization of ecosystems exposed to volcanically elevated CO₂ to detect changes in deep volcanic degassing by using
30 selected species of trees as sensors.

31 **1 Introduction**

32 Tropical forests represent about 40% of terrestrial Net Primary Productivity (NPP) worldwide, store 25% of biomass
33 carbon, and may contain 50% of all species on Earth, but the projected future responses of tropical plants to globally
34 rising levels of CO₂ are poorly understood (Leigh et al., 2004; Townsend et al., 2011). The largest source of uncertainty
35 comes from a lack of understanding of long-term CO₂ fertilization effects in the tropics (Cox et al., 2013). Reducing
36 this uncertainty would significantly improve Earth system models, advances in which would help better constrain
37 projections in future climate models (Cox et al., 2013; Friedlingstein et al., 2013). Ongoing debate surrounds the
38 question of how much more atmospheric CO₂ tropical ecosystems can absorb—the “CO₂ fertilization effect” (Gregory
39 et al., 2009; Kauwe et al., 2016; Keeling, 1973; Schimel et al., 2015).

40 Free Air CO₂ Enrichment (FACE) experiments have been conducted to probe this question, but none have
41 been conducted in tropical ecosystems (e.g. Ainsworth and Long, 2005; Norby et al., 2016). Some studies have used
42 CO₂-emitting natural springs to study plant responses to elevated CO₂, but these have been limited in scope due to the
43 small spatial areas around springs that experience elevated CO₂ (Paoletti et al., 2007; Saurer et al., 2003). These studies
44 have suffered from several confounding influences, including other gas species that accompany CO₂ emissions at
45 these springs, human disturbances, and difficulty with finding appropriate control locations. Additionally, none have
46 been conducted in the tropics (Pinkard et al., 2010). A series of studies in Yellowstone National Park (USA) used its
47 widespread volcanic hydrothermal CO₂ emissions for the same purpose, though it is not in the tropics (Sharma and
48 Williams, 2009; Tercek et al., 2008). Yellowstone was particularly suitable for this type of study, due to its protected
49 status as a National Park, and because the large areas of CO₂ emissions made control points more available (Sharma
50 and Williams, 2009; Tercek et al., 2008). These studies reported changes in rubisco, an enzyme central to CO₂ fixation,
51 and sugar production in leaves similar to results from FACE experiments, suggesting that volcanically-influenced
52 areas like Yellowstone have untapped potential for studying the long-term effects of elevated CO₂ on plants.

53 Tropical ecosystems on the vegetated flanks of active volcanoes offer large and diverse ecosystems that could
54 make this type of study viable. Well over 200 active volcanoes are in the tropics (Global Volcanism Program, 2013)
55 and many of these volcanoes are heavily forested. However, fewer of these tropical volcanic forests have sufficient

56 legal protection to be a source of long-term information, and the effects of diffuse volcanic flank gas emissions on the
57 overlying ecosystems remain largely unknown. Most previous studies focused on extreme conditions, such as tree kill
58 areas associated with extraordinarily high CO₂ emissions at Mammoth Mountain, CA (USA) (Biondi and Fessenden,
59 1999; Farrar et al., 1995; Sorey et al., 1998). However, the non-lethal effects of cold volcanic CO₂ emissions—away
60 from the peak emission zones, but still in the theorized fertilization window—have received little attention, and could
61 offer a new approach to studying the effects of elevated CO₂ on ecosystems (Cawse-Nicholson et al., 2018; Vodnik
62 et al., 2018). The broad flanks of active volcanoes experience diffuse emissions of excess CO₂ because the underlying
63 active magma bodies continuously release gas, dominated by CO₂ transported to the surface along fault lines (Chiodini
64 et al., 1998; Dietrich et al., 2016; Farrar et al., 1995). This process has frequently been studied to understand the
65 dynamics of active magma chambers and to assess potential volcanic hazards (Chiodini et al., 1998; Sorey et al.,
66 1998). These emissions are released through faults and fractures on the flanks of the volcano (Burton et al., 2013;
67 Pérez et al., 2011; Williams-Jones et al., 2000)(see Supplementary Figure S1). Volcanic flanks through which these
68 gases emanate are broad, covering typically 50-200 km², often supporting well-developed, healthy ecosystems. Some
69 of these faults tap into shallow acid hydrothermal aquifers, but by the time these gases reach the surface of most
70 forested volcanoes, soluble and reactive volcanic gas species (e.g., SO₂, HF, HCl, H₂S) have been scrubbed out in the
71 deep subsurface, leading to a diffusely emanated gas mix of predominantly CO₂ with minor amounts of hydrogen,
72 helium, and water vapor reaching the surface (Symonds et al., 2001).

73 Trees in these locations are continuously exposed to somewhat variably elevated levels of CO₂ (eCO₂),
74 though it is unclear if the trees utilize this excess CO₂. Volcanic CO₂ has a heavy δ¹³C signature typically ranging
75 from -7 to -1 ‰, which is distinct from typical vegetation and noticeably heavier than typical atmospheric values
76 (Mason et al., 2017). If trees incorporate volcanic CO₂, then the stable carbon isotopic composition of wood may
77 document the long-term, possibly variable influence of volcanic CO₂ during the tree's growth. With this tracer
78 available, volcanic ecosystems could become a valuable natural laboratory to study the long-term effects of elevated
79 CO₂ on ecosystems, especially in understudied regions like the tropics. Additionally, short-term effects of eCO₂ might
80 be revealed by plant functional measurements at the leaf scale, where the additional CO₂ could increase carbon uptake
81 in photosynthesis.

82 Here we provide preliminary results on the short- and long-term non-lethal impacts of diffuse volcanic CO₂
83 emissions on three species of tropical trees on the flanks of two active volcanoes in Costa Rica. We also explore the
84 viability of studying volcanically-influenced ecosystems to better understand potential future responses to elevated
85 CO₂, and suggest adjustments to our approach that will benefit future, similarly-motivated studies.

86 **2 Methods**

87 **2.1 Investigated locations and sampling strategy**

88 Irazú and Turrialba are two active volcanoes located ~25 and 35 km east of San José, Costa Rica (Fig. 1). These two
89 volcanoes are divided by a large erosional basin. The two volcanoes cover approximately 315 km², which is
90 significantly larger than the average forested active volcanic edifice in Costa Rica at 122 km². The vast majority of

91 the northern flanks of Irazú and Turrialba are covered in legally protected dense old-growth forest, while the southern
92 flanks are dominated by pasture land and agriculture. Turrialba rises 3,300 m above its base and has been active for
93 at least 75,000 years with mostly fumarolic activity since its last major eruption in 1866 (Alvarado et al., 2006). It has
94 experienced renewed activity beginning in 2010, and its current activity is primarily characterized by a near-constant
95 volcanic degassing plume, episodic minor ash emissions, and fumarolic discharges at two of the summit craters, as
96 well as significant diffuse and fumarolic gas emissions across its flanks, focused along fault systems (Martini et al.,
97 2010). Turrialba's CO₂ emissions in areas proximal to the crater were calculated at 113 ± 46 tons/d (Epiard et al.,
98 2017). The Falla Ariete (Ariete fault), a major regional fault, runs northeast-southwest through the southern part of
99 Turrialba's central edifice and is one of the largest areas of diffuse CO₂ emissions on Turrialba (Epiard et al., 2017;
100 Rizzo et al., 2016). Atmospheric CO₂ has an average δ¹³C value of -9.2 ‰ at Turrialba, and the volcanic CO₂ released
101 at the Ariete fault has significantly heavier δ¹³C values clustered around -3.4 ‰ (Malowany et al., 2017).

102 Irazú has been active for at least 3,000 years, and had minor phreato-magmatic eruptions in 1963 and a single
103 hydrothermal eruption in 1994. Currently, Irazú's activity primarily consists of shallow seismic swarms, fumarolic
104 crater gas emissions, small volcanic landslides, and minor gas emissions on its northern forested flank (Alvarado et
105 al., 2006; Barquero et al., 1995). Diffuse cold flank emissions of volcanic CO₂ represent the vast majority of gas
106 discharge from Irazú, as the main crater releases 3.8 t d⁻¹ of CO₂ and a small area on the north flank alone releases 15
107 t d⁻¹ (Epiard et al., 2017). Between the two volcanoes, a major erosional depression is partially occupied by extensive
108 dairy farms, and is somewhat less forested than their flanks.

109 In this study, we focused on accessible areas between 2,000 and 3,300 m on both volcanoes (Fig. 1). On
110 Irazú, we sampled trees and CO₂ fluxes from the summit area to the north, near the approximately north-south striking
111 Rio Sucio fault, crossing into the area dominated by dairy farms on Irazú's lower northeastern slope. Of significant
112 importance for this type of study is that all active volcanoes on Earth continuously emit CO₂ diffusely through fractures
113 and diffuse degassing structures on their flanks, at distances hundreds to thousands of meters away from the crater
114 (Dietrich et al., 2016; Epiard et al., 2017), and this elevated CO₂ degassing persists continuously and consistently over
115 decades to centuries (Burton et al., 2013; Delmelle and Stix, 1999; Nicholson, 2017). There is no inherent seasonal or
116 meteorological variability of the source gas pressure, and no dependence on shallow soil or vegetation chemistry or
117 biology (though increased soil moisture in the rainy season, wind, and atmospheric pressure can modulate gas
118 permeability of the shallow soil) (Camarda et al., 2006). The soil overlying deep reaching fracture systems acts as a
119 diffuser through which the volcanic gas percolates and enters the sub-canopy air. For our study sites, portions of the
120 volcanoes with active "cold" CO₂ degassing have already been assessed and mapped previously (Epiard et al., 2017;
121 Malowany et al., 2017).

122 Our sampling locations on Irazú were located along a road from the summit northward down into this low-
123 lying area. On Turrialba, we focused on an area of known strong emissions but intact forests on the SW slope, uphill
124 of the same erosional depression, but cross-cut by the major NE-SW trending active fracture system of the Falla Ariete.
125 We sampled three main areas of the Falla Ariete, each approximately perpendicularly transecting the degassing fault
126 along equal altitude; the upper Ariete fault, the lower Ariete fault, and a small basin directly east of the old Cerro
127 Armado cinder cone on Turrialba's south-western flank. We took a total of 51 tree samples (17 were excluded after

128 stress screening) at irregular intervals depending on the continued availability and specimen maturity of three species
129 present throughout the transect.

130 All transects are in areas experiencing measurable CO₂ enhancements from the Falla Ariete, but not high
131 enough in altitude to be in areas generally downwind of the prevailing crater emissions plume (Epiard et al., 2017).
132 We avoided areas that experience ash fall, high volcanic SO₂ concentrations, local anthropogenic CO₂ from farms, or
133 that were likely to have heavily acidified soil. Excessively high soil CO₂ concentrations can acidify soil, leading to
134 negative impacts on ecosystems growing there (McGee and Gerlach, 1998). Because such effects reflect by-products
135 of extreme soil CO₂ concentrations rather than direct consequences of elevated CO₂ on plants, we avoided areas with
136 CO₂ fluxes high enough to possibly cause noticeable CO₂-induced soil acidification. Light ash fall on some days likely
137 derived from atmospheric drift, as we were not sampling in areas downwind of the crater. The ash fall did not in any
138 noticeably way affect our samples, as trees showing ash accumulation on their leaves or previous damage were the
139 exception and avoided. Altitude, amount of sunlight during measurements, and aspect had no consistent correlations
140 with any of the parameters we measured.

141 **2.2 Studied tree species**

142 Our study focused on three tree species found commonly on Turrialba and Irazú: *Buddleja nitida*, *Alnus acuminata*,
143 and *Oreopanax xalapensis*. *B. nitida* is a small tree with a typical stem diameter (DBH) ranging from 5 to 40 cm that
144 grows at elevations of 2,000-4,000 m throughout most of Central America (Kappelle et al., 1996; Norman, 2000). The
145 DBH of the individuals we measured ranged from 11.5 to 51.3 cm, with an average of 29.85 cm. It averages 4-15 m
146 in height and grows primarily in early and late secondary forests (Kappelle et al., 1996; Norman, 2000). *A. acuminata*
147 is a nitrogen-fixing pioneer species exotic to the tropics that can survive at elevations from 1,500-3,400 m, although
148 it is most commonly found between 2,000-2,800 m (Weng et al., 2004). The trees we measured had DBH ranging
149 from 14.3 to 112 cm, with an average of 57.14 cm. *O. xalapensis* thrives in early and late successional forests, although
150 it can survive in primary forests as well (Kappelle et al., 1996; Quintana-Ascencio et al., 2004). It had the smallest
151 average DBH of the three species, ranging from 6.6 to 40.9 cm, with an average of 22.71 cm.

152 **2.3 CO₂ concentrations and soil diffuse flux measurements**

153 Soil CO₂ flux was measured with an accumulation chamber near the base of the tree (generally within 5 meters, terrain
154 permitting) at three different points and then averaged to provide a single CO₂ flux value to compare to the ¹³C
155 measurement of the corresponding tree sample. This technique is intended to provide a simple relative way to compare
156 the CO₂ exposure of different trees, as a tree with high CO₂ flux near its base should experience consistently higher
157 CO₂ concentrations than a tree with lower CO₂ flux. We also measured concentrations at ground level and 1.5 – 2.0
158 m above ground level, though these were expectedly highly variable in time and location. We analyzed CO₂ fluxes,
159 not concentrations, because the diffuse emissions of excess volcanic CO₂ through the soil, fed from a deep magma
160 source and location-dependent on constant deep geological permeability, are highly invariant in time compared to
161 under-canopy air concentrations. In contrast, instantaneous concentration measurements in the sub-canopy air are
162 modulated by many factors including meteorology, respiration of vegetation and animals, uptake by plants for

163 photosynthesis, and diurnal dynamic and slope effects. An approach of instantaneous highly variable concentration
164 measurements is thus not representative of long-term exposure. The approach of measuring the largely invariant soil-
165 to-atmosphere volcanic CO₂ fluxes is much more representative of long-term exposure, varying mostly spatially and
166 the site-to-site differences are therefore more representative of the lifetime of exposure of the trees.

167
168 We used a custom-built soil flux chamber system which contained a LI-COR 840A non-dispersive infrared CO₂ sensor
169 (LI-COR Inc., Lincoln NE, USA) to measure soil CO₂ flux. A custom-built cylindrical accumulation chamber of
170 defined volume was sealed to the ground and remained connected to the LI-COR sensor. The air within the
171 accumulation chamber was continuously recirculated through the sensor, passing through a particle filter. The sensor
172 was calibrated before deployment and performed within specifications. We recorded cell pressure and temperature,
173 ambient pressure, air temperature, GPS location, time stamps, location description, wind speed and direction, relative
174 humidity, and slope, aspect, and altitude as ancillary data. In typical operation, each measurement site for flux
175 measurements was validated for leaks (visible in the live data stream display as spikes and breaks in the CO₂
176 concentration slope), and potential external disturbances were avoided (such as vehicle traffic, generators, or breathing
177 animals and humans). Measurements were recorded in triplicate for at least 2 minutes per site. Data reduction was
178 performed using recorded time stamps in the dataset, with conservative time margins to account for sensor response
179 dead time, validated against consistent slope sections of increasing chamber CO₂. Fluxes were computed using
180 ancillary pressure and temperature measurements and the geometric chamber constant (chamber volume at inserted
181 depth, tubing volume, and sensor volume). Care was taken to not disturb the soil and overlying litter inside and
182 adjacent to, the chamber.

183 **2.4 Leaf function measurements**

184 Chlorophyll fluorescence measurements were conducted on leaves of all three species during the field campaign to
185 obtain information on instantaneous plant stress using an OS30p+ fluorometer (Opti-Sciences Inc., Hudson, NH,
186 USA). Five mature leaves from each individual tree were dark adapted for at least 20 minutes to ensure complete
187 relaxation of the photosystems. After dark adaptation, initial minimal fluorescence was recorded (F_0) under conditions
188 where we assume that photosystem II (PSII) was fully reduced. Immediately following the F_0 measurement, a 6,000
189 $\mu\text{mol m}^{-2} \text{s}^{-1}$ saturation pulse was delivered from an array of red LEDs at 660 nm to record maximal fluorescence
190 emission (F_m), when the reaction centers are assumed to be fully closed. From this, the variable fluorescence was
191 determined as $F_v/F_m = (F_m - F_0)/F_m$. F_v/F_m is a widely used chlorophyll fluorescence variable used to assess the
192 efficiency of PSII and, indirectly, plant stress (Baker and Oxborough, 2004). The five F_v/F_m measurements were
193 averaged to provide a representative value for each individual tree. Some trees had less than five measurements due
194 to the dark adaptation clips slipping off the leaf before measurements could be taken. Ten trees had four measurements,
195 and another six had three measurements

196 Chlorophyll concentration index (CCI) was measured with a MC-100 Apogee Instruments chlorophyll
197 concentration meter (Apogee Instruments, Inc., Logan, UT, USA). CCI was converted to chlorophyll concentration
198 ($\mu\text{mol m}^{-2}$) with the generic formula derived by Parry et al., 2014. Depending on availability, between three and six

199 leaves were measured for CCI for each tree, and then averaged to provide a single value for each tree. If leaves were
200 not within reach, a branch was pulled down or individual leaves were shot down with a slingshot and collected.
201 Photosynthetically active radiation was measured at each tree with a handheld quantum meter (Apogee Instruments,
202 Logan, UT, USA) (Table S2). Stomatal conductance to water vapor, g_s ($\text{mmol m}^{-2} \text{s}^{-1}$) was measured between 10:00-
203 14:00 hours using a steady-state porometer (SC-1, Decagon Devices, Inc., Pullman, WA, USA), calibrated before use
204 and read in manual mode. This leaf porometer was rated for humidity <90%, and humidity was sometimes above this
205 limit during our field work. Consequently, we have fewer stomatal conductance measurements than our other data
206 types.

207 **2.5 Isotopic analysis**

208 We collected wood cores from 31 individual trees at a 1.5 m height using a 5.15 mm diameter increment borer (JIM
209 GEM, Forestry Suppliers Inc., Jackson, MS, USA). Since no definable tree rings were apparent, we created a fine
210 powder for isotope analysis by drilling holes into dried cores using a dry ceramic drill bit (Dremel) along the outermost
211 5 cm of wood below the bark, which was chosen to represent the most recent carbon signal for ^{13}C analyses. The fine
212 powder (200 mesh, 0.2 – 5 mg) was then mixed and a random sample was used to extract $^{13}\text{C}/^{12}\text{C}$ ratios (to obtain
213 $\delta^{13}\text{C}$ values against the VPDB standard), which we estimated to be representative of at least the last 2-3 years, based
214 on analogous literature growth rate values: *O. xalapensis* and *A. acuminata* range from 0.25 - 2.5 cm/y and 0.6 - 0.9
215 cm/y, respectively (Kappelle et al., 1996; Ortega-Pieck et al, 2011). These rates result in a 5 cm range of at least 2 and
216 5.5 years, though the high rates were determined for very young trees under very different conditions and it is explicitly
217 unknown in our study. Since we only sample the most recent years, no isotopic discrimination against atmospheric
218 ^{13}C due to preferential diffusion and carboxylation of ^{12}C , was conducted. Rather, we assume that $\delta^{13}\text{C}$ values are
219 representative of the relative amount of volcanic CO_2 vs. atmospheric CO_2 sequestered by the tree over the period of
220 growth represented in the sample. $\delta^{13}\text{C}$ values were determined by continuous flow dual isotope analysis using a
221 CHNOS Elemental Analyzer and IsoPrime 100 mass spectrometer at the University of California Berkeley Center for
222 Stable Isotope Biogeochemistry. External precision for C isotope determinations is ± 0.10 ‰. Ten $\delta^{13}\text{C}$ measurements
223 did not have corresponding soil CO_2 flux measurements due to the flux measurements being unavailable for the final
224 two days of sampling, and another 5 samples were from trees that showed signs of extreme stress, such as browning
225 leaves or anomalously low fluorescence measurements. Since the purpose of our study was to explore the non-lethal
226 effects of volcanic CO_2 on trees, during analysis we excluded all trees that were observed in the field to show visible
227 signs of stress, or that were not fully mature. After these exclusions, all remaining tree cores with co-located CO_2 flux
228 measurements were from Turrialba.

229 **2.6 Sulfur dioxide probability from satellite data**

230 To assess the likelihood of trees having been significantly stressed in the past by volcanic sulfur dioxide (SO_2) from
231 the central crater vents, we took two approaches. First, we were guided by in-situ measurements taken in the same
232 areas by Jenkins et al. (2012), who assessed the physiological interactions of SO_2 and CO_2 on vegetation on the upper
233 lobes of Turrialba and demonstrated a rapid exponential decay of SO_2 away from the central vent. Second, for long-

234 term exposure we derived the likelihood of exposure per unit area using satellite data sensitive to SO₂ (Fig. 2). The
235 Advanced Spaceborne Thermal Emission and Reflection Radiometer (ASTER), launched in December 1999 on
236 NASA's Terra satellite, has bands sensitive to SO₂ emission in the thermal infrared (TIR), at ~60 m x 60 m spatial
237 resolution. We initially used ASTER Surface Radiance TIR data (AST_09T), using all ASTER observations of the
238 target area over the entirety of the ASTER mission (October 2000 until writing in late 2017). The TIR bands were
239 corrected for downwelling sky irradiance and converted into units of W m⁻² μm⁻¹. For each observation, an absorption
240 product is calculated by subtracting SO₂-insensitive from SO₂-sensitive bands:

$$241 \quad S^t = (b_{10} + b_{12}) - 2 \cdot b_{11} \quad (1)$$

242 Where S is the SO₂ index, t is an index representing the time of acquisition, b_{10} is the radiance at band 10 (8.125 -
243 8.475 μm), b_{11} is the radiance at band 11 (8.475 - 8.825 μm), and b_{12} is the radiance at band 12 (8.925 - 9.275 μm).
244 This is similar to the method of Campion et al., 2010. The granules were then separated into day and night scenes,
245 projected onto a common grid, and then thresholded to $S > 0.1 \text{ W m}^{-2} \mu\text{m}^{-1}$, and converted into a probability. The
246 output is a spatial dataset that describes the probability of an ASTER observation showing an absorption feature above
247 a $0.1 \text{ W m}^{-2} \mu\text{m}^{-1}$ threshold across the entirety of the ASTER observations for day or night separately. The number of
248 scenes varies per target, but they tend to be between 200-800 observations in total, over the 17 year time period of
249 satellite observations. However, certain permanent features, such as salt pans, show absorption features in band 11
250 and therefore have high ratios for the algorithm used. We therefore used a second method that seeks to map transient
251 absorption features. For this method, we subtract the median from each S^t , yielding a median deviation stack. By
252 plotting the maximum deviations across all observations, we then get a map of transient absorption features, in our
253 case this is mostly volcanic SO₂ plumes, which map out the cumulative position of different plume observations well.
254 To speed up processing, some of the retrieval runs were binned in order to increase the signal-to-noise ratio, since the
255 band difference can be rather noisy.

256 **2.7 Modelling the anthropogenic CO₂ influence from inventory data**

257 We assessed the likelihood of anthropogenic CO₂, enhancements of air from San Jose, Costa Rica's capital and main
258 industrial and population center, influencing our measurements. We used a widely applied Flexible Particle Dispersion
259 Model (Eckhardt et al., 2017; Stohl et al., 1998, 2005; Stohl and Thomson, 1999) in a forward mode (Stohl et al.,
260 2005), Flexpart, to simulate the downwind concentrations of CO₂ in the atmosphere (e.g., Belikov et al., 2016), due
261 to inventory-derived fossil fuel (FF) emissions in our study area for the year 2015 (Fig. 2). The National Centers for
262 Environmental Prediction (NCEP) - Climate Forecast System Reanalysis (CFSR) 2.5° horizontal resolution
263 meteorology (Saha et al., 2010b, 2010a), and 1-km Open-Source Data Inventory for Anthropogenic CO₂ (ODIAC;
264 Oda and Maksyutov, 2011) emissions for 2015 were used to drive the Flexpart model. The CO₂ concentrations were
265 generated at a 1 km spatial resolution within three vertical levels of the atmosphere (0-100, 100-300, 300-500 meters)
266 that are possibly relevant to forest canopies in Costa Rica. However, to assess the magnitude of enhancements we only
267 used CO₂ concentrations observed within the lowest modelled level of the atmosphere, from 0-100 meters. Validation
268 of the model with direct observations was not required because we were only interested in ensuring that anthropogenic
269 CO₂ dispersed upslope from San José was not having a significant effect on our study area, we were not aiming to

270 capture intra-canopy variability, typically at tens to hundreds of ppm variable, which is not relevant to the better
271 mixed, distal single-digit or less ppm signal from San Jose. The actual concentration of CO₂ and any biogenic influence
272 in the modelled area was irrelevant because the spatial distribution of anthropogenic CO₂ was the only factor relevant
273 for this test. 2015 was used as a representative year for simulating the seasonal cycle of CO₂ concentrations that would
274 be present in any particular year.

275 **3 Results**

276 **3.1 Volcanic CO₂ emissions through the soil**

277 We measured CO₂ flux emitted through the soil at 66 points over four days (Fig. 1). The first eight points were on
278 Irazú, and the rest were located near the Ariete fault on Turrialba. Mean soil CO₂ flux values over the entire sampling
279 area varied from 3 to 37 g m⁻² day⁻¹, with an average of 11.6 g m⁻² day⁻¹ and a standard deviation of 6.6 g m⁻² day⁻¹. A
280 12-bin histogram of mean CO₂ flux shows a bimodal right-skewed distribution with a few distinct outliers (Fig. 3).
281 Fluxes were generally larger on Irazú than on Turrialba. This result agrees with previous studies which showed that
282 the north flank of Irazú has areas of extremely high degassing, whereas most of our sampling locations on Turrialba
283 were in areas that had comparatively lower diffuse emissions (Epiard et al., 2017; Stine and Banks, 1991). We used a
284 cumulative probability plot to identify different populations of CO₂ fluxes (Fig. 3) (Cardellini et al., 2003; Sinclair,
285 1974).

286 We created an inventory-based model of anthropogenic CO₂ emissions from the San José urban area, parts
287 of which are less than 15 km from some of our sampling locations (Fig. 2). Our model shows that CO₂ emitted from
288 San José is blown west to south-west by prevailing winds. Our study area is directly east of San José, and as such is
289 unaffected by anthropogenic CO₂ from San Jose, which is the only major urban area near Turrialba and Irazú. Since
290 the trees sampled are spatially close to each other, they are exposed to the same regional background CO₂ variability.
291 Additionally, we used ASTER data to map probabilities of SO₂ across Costa Rica, as a possible confounding factor.
292 The active craters of both Turrialba and Irazú emit measurable amounts of SO₂, which is reflected by the high SO₂
293 probabilities derived there (Fig. 2). Tropospheric SO₂ quickly converts to sulfate, a well-studied process intensified
294 by the presence of volcanic mineral ash, plume turbulence, and a humid tropical environment (Oppenheimer et al.,
295 1989; Eatough et al., 1994); furthermore, the bulk of the SO₂ emissions is carried aloft. Consequently, any remaining
296 SO₂ causing acid damage effects on trees at Turrialba is limited to a narrow band of a few 100 m around the mostly
297 quietly steaming central vent, which has been thoroughly ecologically evaluated for acid damage (Jenkins et al., 2012).
298 D’Arcy (2018) has assessed this narrow, heavily SO₂-affected area immediately surrounding the central crater vent of
299 Turrialba, which we avoided, and our sampling sites are mostly within their control zone not considered majorly
300 affected by SO₂, but where diffuse CO₂ degassing dominates the excess gas phase (Epiard et al, 2017). Our study area
301 is on the flanks of the volcano, where ASTER-derived SO₂ probability is minimal, and SO₂ influence not detectable
302 on the ground (Jenkins et al., 2012; Campion et al., 2012). Most other volcanoes in Costa Rica emit little to no SO₂
303 on a decadal time scale, shown by the low or non-existent long-term SO₂ probabilities over the other volcanoes in
304 Costa Rica (white polygons in Fig. 2).

305 3.2 Tree core isotopes

306 Bulk wood $\delta^{13}\text{C}$ measurements of all samples in this study, independent of exposure, ranged from -24.03 to -28.12
307 ‰, with most being clustered around -26 ‰ (Fig. 4). A 5-bin histogram of all $\delta^{13}\text{C}$ measurements shows a slightly
308 right-skewed unimodal normal distribution, with an average of -26.37 ‰ and a standard deviation of 0.85 ‰. *A.*
309 *acuminata* and *O. xalapensis* have nearly identical averages (-26.14 and -25.97 ‰, respectively), while *B. nitida* has
310 a noticeably lighter average of -27.02 ‰. Diffuse excess CO_2 emissions throughout the investigation areas reflect a
311 deep volcanic source which typically varies little in time (Epiard et al., 2017), but such diffuse emissions spatially
312 follow geological subsurface structures (Giammanco et al., 1997). Their temporal variability therefore reflects long-
313 term low-amplitude modulation of the volcanic heavy- $\delta^{13}\text{C}$ signal, and their spatial distribution is mostly constant
314 over tree lifetimes (Aiuppa et al., 2004; Peiffer et al., 2018; Werner et al., 2014), providing a constant long-term spatial
315 gradient of CO_2 exposure to the forest canopy. Our data show that in areas where CO_2 flux is higher, the wood cores
316 contained progressively higher amounts of ^{13}C for two of the three species. Interestingly, our tree core $\delta^{13}\text{C}$ showed
317 no relationship with instantaneous stomatal conductance for any species, indicating that no stress threshold was
318 exceeded during measurement across the sample set.

319 3.3 Plant function (Fluorescence, Chlorophyll, Stomatal Conductance)

320 Our measurements and literature data confirm that ecosystems growing in these locations are consistently exposed to
321 excess volcanic CO_2 , which may impact chlorophyll fluorescence, chlorophyll concentrations, and stomatal
322 conductance of nearby trees. After excluding visibly damaged trees, leaf fluorescence, expressed as F_v/F_m , was very
323 high in most samples. F_v/F_m ranged from 0.75 to 0.89, with most measurements clustering between 0.8 and 0.85
324 (Fig. 5). The fluorescence data has a left-skewed unimodal distribution. The leaf fluorescence (F_v/F_m) values for *A.*
325 *acuminata* had a strong positive correlation with soil CO_2 flux ($r^2=0.69$, $p<.05$), while the other two species showed
326 no correlation. No confounding factors measured were correlated with F_v/F_m for any species. In general, *B. nitida*
327 had the highest F_v/F_m values, and *A. acuminata* and *O. xalapensis* had similar values except for a few *O. xalapensis*
328 outliers. Chlorophyll concentration measurements were highly variable, ranging from 260 to 922 $\mu\text{mol m}^{-2}$, with an
329 average of 558 $\mu\text{mol m}^{-2}$ and a standard deviation of 162 $\mu\text{mol m}^{-2}$ (Fig. 6). Chlorophyll concentration had a
330 complicated right-skewed bimodal distribution, likely due to the noticeably different averages for each species. *A.*
331 *acuminata* and *O. xalapensis* both displayed weak correlations between chlorophyll concentration and soil CO_2 flux
332 ($r^2=0.38$ and $r^2=0.28$, respectively), but their trendlines were found to be almost perpendicular (Fig. 6). As CO_2 flux
333 increased, *A. acuminata* showed a slight increase in chlorophyll concentration, while *O. xalapensis* had significant
334 decreases in chlorophyll concentration. *B. nitida* individuals growing on steeper slopes had significantly lower
335 chlorophyll concentration measurements ($r^2=0.42$, $p<.05$) than those on gentler slopes, a trend not expressed by either
336 of the other two species ($r^2=0.01$ for both), demonstrating no significant influence of slope across the majority of
337 samples. Stomatal conductance ranged from 83.5 to 361 $\text{mmol H}_2\text{O m}^{-2} \text{s}^{-1}$, with an average of 214 $\text{mmol H}_2\text{O m}^{-2} \text{s}^{-1}$
338 and a standard deviation of 73.5 $\text{mmol H}_2\text{O m}^{-2} \text{s}^{-1}$. Distribution was bimodal, with peaks around 150 and 350
339 $\text{mmol H}_2\text{O m}^{-2} \text{s}^{-1}$. *A. acuminata* had a moderate positive correlation ($r^2=0.51$) with soil CO_2 flux, but it was not
340 statistically significant due to a lack of data points (Fig. 7) – however this is a result consistent with the observed

341 higher chlorophyll concentration (Fig. 6). The other two species displayed no correlation with soil CO₂ flux. *B. nitida*
342 had a moderate negative correlation ($r^2=0.61$) with slope, similar to its correlation between chlorophyll concentration
343 and slope.

344 **4 Discussion**

345 **4.1 Long-term plant uptake of volcanic CO₂**

346 Turrialba and Irazú continuously emit CO₂ through their vegetated flanks, but prior to this study it was unknown if
347 the trees growing there were utilizing this additional isotopically heavy volcanic CO₂. All tree cores with
348 corresponding CO₂ flux measurements were from areas proximal to the Ariete fault on Turrialba, where atmospheric
349 and volcanic δ¹³C have significantly different values (-9.2 and -3.4 ‰, respectively) (Malowany et al., 2017). If the
350 trees assimilate volcanic CO₂ through their stomata, then we would expect wood δ¹³C to trend towards heavier values
351 as diffuse volcanic CO₂ flux increases. After excluding damaged samples and stressed trees, δ¹³C was strongly
352 correlated with soil CO₂ flux for both *B. nitida* and *O. xalapensis* (Fig. 4). *A. acuminata* did not have a statistically
353 significant correlation between soil CO₂ flux and δ¹³C, likely because it had the fewest data points and a minimal
354 range of CO₂ and δ¹³C values. The difference in regression slope between *B. nitida* and *O. xalapensis* (Fig. 4) may be
355 due to physiological differences across traits or species, and/or due to differences in exposure owing to canopy height
356 differences. Resolving this question would require a much larger multi-species sample size which could only be
357 sufficiently obtained using remote sensing methods. The strong positive correlations between CO₂ flux and
358 increasingly heavy δ¹³C values suggest that the trees have consistently photosynthesized with isotopically heavy
359 excess volcanic CO₂ over the last few years, and are therefore growing in eCO₂ conditions. Assuming that most of the
360 variations in δ¹³C are caused by incorporation of heavy volcanic CO₂, we can calculate the average concentration of
361 the mean volcanic excess CO₂ in the air the plants are exposed to, with a mass balance equation (Eq. 2):

$$362 \quad C_v = \frac{(\delta_b - \delta_t)}{(\delta_a - \delta_v)} C_a \quad (2)$$

363 where C_v is the mean volcanic excess component of the CO₂ concentration in air, C_a is the atmospheric “background”
364 (i.e., non-volcanic) CO₂ concentration, δ_a is atmospheric δ¹³C, δ_b is the most negative δ¹³C measurement for the species
365 being studied, δ_t is the δ¹³C value for the tree that volcanic CO₂ exposure is being calculated, and δ_v is δ¹³C of the
366 volcanic CO₂. Background wood δ¹³C is the value of the point for each species with the lowest CO₂ flux (Fig. 4), and
367 the other wood δ¹³C measurement is any other point from the same species. Values for δ_v , δ_a , and C_a are taken from
368 Malowany et al., 2017. For the tree core with the highest measured CO₂ flux for *O. xalapensis*, this equation yields a
369 mean excess volcanic CO₂ concentration of 115 ppm, bringing the combined mean atmospheric (including volcanic)
370 CO₂ concentration tree exposure to potentially around ~520 ppm. For *B. nitida* this equation yields 133 ppm of mean
371 excess volcanic CO₂ at the highest flux location, for a combined total mean of potentially ~538 ppm CO₂. These
372 numbers may be on the high side as the calculation assumes that carbon isotope discrimination remains constant for
373 all trees within a given species, but they serve as estimate of the approximate magnitude of the average amount of
374 CO₂ that these trees are exposed to. A tree ring study at Mammoth Mountain found an average yearly volcanic excess
375 CO₂ exposure of 20-70 ppm over a 15-year period (Lewicki et al., 2014). Turrialba is significantly more active than

376 Mammoth Mountain, so trees growing in high emission areas of Turrialba may be exposed to similar or higher amounts
377 of CO₂ than the tree in the Mammoth Mountain study. Additional measurements of tree core δ¹³C and associated soil
378 CO₂ fluxes would help corroborate our observations, which were based on a limited number of data points. Though
379 tree ring ¹⁴C content in volcanically active areas has been linked to variations in volcanic CO₂ emissions, and
380 comparing patterns of δ¹³C to ¹⁴C measurements for the same wood samples could provide additional confirmation of
381 this finding (Evans et al., 2010; Lefevre et al., 2017; Lewicki et al., 2014), this additional dimension was outside the
382 scope of this exploratory study. However, beyond such pattern confirmation, using ¹⁴C dating of trees exposed to
383 naturally isotopically distinct excess CO₂ is, in fact, unfortunately not a reliable method for these environments due
384 to the well-known δ¹⁴C deficiency in trees exposed to excess volcanic CO₂ which is isotopically “dead” with respect
385 to ¹⁴C, creating spurious patterns that preclude dating by ¹⁴C (e.g., Lefevre et al., 2017; Lewicki et al., 2014).

386 Our data demonstrate that CO₂ fluxes through the soil may be a representative relative measure for eCO₂
387 exposure of overlying tree canopies. Forest canopy exposure to volcanic CO₂ will vary over time, as will volcanic
388 eCO₂, once emitted through the soil into the sub-canopy atmosphere, the gas experiences highly variable thermal and
389 wind disturbances which significantly affect dispersion of CO₂ on minute to minute, diurnal, and seasonal timescales
390 (Staebler and Fitzjarrald, 2004; Thomas, 2011). These processes cause in-canopy measurements of CO₂ concentration
391 to be highly variable, making instantaneous concentration measurements in a single field campaign not representative
392 of long-term relative magnitudes of CO₂ exposure. Soil CO₂ fluxes are less tied to atmospheric conditions, and are
393 primarily externally modulated by rainfall which increases soil moisture and therefore lowers the soil’s gas
394 permeability (Camarda et al., 2006; Viveiros et al., 2009). These fluxes can also be affected by variations in barometric
395 pressure, but both of these factors are easily measurable and therefore can be factored in when conducting field work
396 (Viveiros et al., 2009). Assuming the avoidance of significant rainfall and pressure spikes during sampling
397 (measurements were conducted in the dry season and no heavy rains or significant meteorological variations in
398 pressure occurred during field work), measuring the input of CO₂ into the sub-canopy atmosphere as soil CO₂ fluxes
399 is therefore expected to better represent long-term input and exposure of tree canopies to eCO₂ than direct
400 instantaneous measurements of sub-canopy CO₂ concentration. Previous studies at Turrialba have shown that local
401 volcanic CO₂ flux is relatively constant on monthly to yearly timescales (de Moor et al., 2016). Therefore, current soil
402 CO₂ fluxes should give relatively accurate estimates of CO₂ exposure over time. This paper corroborates that
403 expectation by demonstrating strong spatial correlations between volcanically enhanced soil CO₂ emissions with co-
404 located stable carbon isotope signals of these emissions documented in the trees’ xylem.

405 A study at the previously mentioned Mammoth Mountain tree kill area examined the connection between
406 δ¹³C and volcanic CO₂ fluxes, but focused on the difference between trees killed by extreme CO₂ conditions and those
407 that were still alive (Biondi and Fessenden, 1999). They concluded that the changes in δ¹³C that they observed were
408 due to extreme concentrations of CO₂ (soil CO₂ concentrations of up to 100%) impairing the functioning of root
409 systems, leading to closure of stomata and water stress (Biondi and Fessenden, 1999). CO₂ does not inherently harm
410 trees, but the extreme CO₂ concentrations (up to 100% soil CO₂) at the Mammoth Mountain area caused major soil
411 acidification, which led to the tree kill (McGee and Gerlach, 1998). We have evidence that those acidification
412 processes are not affecting our δ¹³C measurements, and that variations in our δ¹³C measurements are more likely to

413 be caused by direct photosynthetic incorporation of isotopically heavy volcanic CO₂. Our δ¹³C measurements have no
414 statistically significant correlation with stomatal conductance, which suggests that our heavier δ¹³C measurements are
415 not linked to stomatal closure. None of the trees included in the analysis (displayed obvious signs of stress, from water
416 or other factors, as indicated by their high fluorescence and chlorophyll concentration values and lack of visible
417 indicators of stress; specifically, our values of Fv/Fm ~0.8 indicate that PSII was operating efficiently in most of the
418 trees we measured (Baker and Oxborough, 2004). The Mammoth Mountain tree kill areas have several orders of
419 magnitude higher CO₂ fluxes (well over 10,000 g m⁻² day⁻¹) than the areas we sampled (up to 38 g m⁻² day⁻¹), making
420 it much more likely that stress from soil acidification would be causing stomatal closure and affecting wood δ¹³C
421 measurements at Mammoth Mountain (Biondi and Fessenden, 1999; McGee and Gerlach, 1998; Werner et al., 2014).
422 In contrast, most of the diffuse degassing at Turrialba does not lead to soil acidification or pore space saturation, as is
423 evident in our own and others' field data (e.g., Epiard et al 2017). Thus, changes in our δ¹³C values are best explained
424 by direct photosynthetic incorporation of isotopically heavy volcanic CO₂. To the best of our knowledge, this is the
425 first time that a direct correlation between volcanic soil CO₂ flux and wood δ¹³C has been documented. Future studies
426 should explore this correlation further, as our findings are based on a limited sample size.

427 **4.2 Short-term species response to eCO₂**

428 Short-term plant functional responses at the leaf level to elevated CO₂ were highly species-dependent. *B. nitida* had
429 no statistically significant functional responses to soil CO₂ flux and *O. xalapensis* only had a weak negative correlation
430 between soil CO₂ flux and chlorophyll concentration (Fig. 6.). *A. acuminata*, a nitrogen fixing species, was the only
431 species with a consistent and positive functional response to elevated CO₂, displaying a strong positive correlation
432 with fluorescence and a weak positive correlation with chlorophyll concentration and stomatal conductance (Figs. 5-
433 7). The lack of response in *B. nitida* and *O. xalapensis* could be due to nitrogen limitation, a factor that would not
434 affect *A. acuminata* due to its nitrogen fixing capability. Previous studies have found that nitrogen availability strongly
435 controls plant responses to eCO₂ in a variety of ecosystems, including grasslands and temperate forests (Garten et al.,
436 2011; Hebeisen et al., 1997; Lüscher et al., 2000; Norby et al., 2010). Nitrogen limitation has been posited to be an
437 important factor in tropical montane cloud forests, and may be contributing to the lack of responses in *B. nitida* and
438 *O. xalapensis* (Tanner et al., 1998). Due to the exploratory nature of our study, we do not have a large enough dataset
439 to conclude that the nitrogen fixing capability of species like *A. acuminata* is the cause for its positive response to
440 volcanically elevated CO₂, as has been speculated before (Schwandner et al., 2004), but it is a possible correlation that
441 deserves further investigation.

442 **4.3 Time constraints**

443 To support these results, we further assessed the possibility of effects of time constraints on growth rates and isotopic
444 signals, despite the compelling spatial variability of the independent variable (naturally isotopically labelled excess
445 volcanic CO₂) in our study (Helle and Schleser, 2004; Verheyden et al., 2004). As tropical trees typically lack tree
446 rings, it is difficult to directly constrain the precise time period that the data represent. However, since we sampled
447 from the outside in, all of the samples appear to at least have the most recent growth period in common. To assess

448 how far back in time our samples could likely represent, we compared our sampled core depths to reported growth
449 rates for the same species in similar environments. Reported growth rates for two of our species, *O. xalapensis* and *A.*
450 *acuminata*, range from 0.25 - 2.5 cm y⁻¹ and 0.6 - 0.9 cm y⁻¹, respectively (Kappelle et al., 1996; Ortega-Pieck et al.,
451 2011). Given that our samples are bulk measurements of the outer 5 cm of wood, each sample would represent between
452 2 and 5.5 years, although the conditions that these growth rates were measured in were different than in our study.
453 Clear time constraints would be necessary for higher resolution analysis, but this need is somewhat mitigated by the
454 continuous, long-term, and over multiple decades mostly invariant nature of diffuse volcanic CO₂ emissions, which is
455 completely independent of any non-volcanic environmental influences on growth rates. By providing an upper and
456 lower bound in the expected growth span represented in our samples, we believe that these samples represent similar
457 time frames during the continuous exposure to excess volcanic CO₂ over the lifetimes of the trees sampled. Due to the
458 continuous nature of the volcanic CO₂ enhancement, we are not investigating and analyzing transient events, but our
459 results instead represent spatial variability in excess CO₂ availability, averaged over similar time periods.

460
461 Although we do not believe our samples represent a long enough time period for long term variations in $\delta^{13}\text{C}$ (Seuss
462 effect) to be relevant, if it does affect our samples it would be beneficial for detection of volcanic CO₂ as the Seuss
463 effect is gradually increasing the gap between atmospheric and volcanic $\delta^{13}\text{C}$. Since our $\delta^{13}\text{C}$ values likely represent
464 several years of growth, small scale temporal variations in excess volcanic CO₂ release are unlikely to significantly
465 impact the results. Larger trees tend to grow slower than smaller trees, so the outer 5 cm of wood should represent a
466 longer time period on larger trees. Thus, if temporal variations had a significant effect on our $\delta^{13}\text{C}$ measurements, we
467 would expect this to be represented by some correlation between DBH and $\delta^{13}\text{C}$, which is not present for any species
468 studied. Three of the five *B. nitida* individuals measured were very large (150-190 cm DBH), whereas the other two
469 are much smaller (11.5 and 15.3 cm DBH). Although the age and growth rates of these two groups of trees likely vary
470 significantly, we found no correlation between DBH and $\delta^{13}\text{C}$; though we did find a strong correlation between the
471 completely independent diffuse excess (volcanic) CO₂ flux and wood $\delta^{13}\text{C}$. Furthermore, the relationships presented
472 are on a per species basis to avoid complications resulting from different growth rates across species. This is important
473 because $\delta^{13}\text{C}$ values provide an integral value of assimilated carbon by the entire tree (not just individual leaves). The
474 depth of tree core sample was identical for each species (the outermost part of the trunk) and we can safely assume
475 that the volcanic CO₂ exposure has been consistent over the time period under investigation.

476
477 Because individual time variability of growth rates can possibly affect these signals as well, future studies that attempt
478 to study tree ring isotopes in this context at higher resolutions will likely require stricter and more detailed time
479 constraints and cell-level stress analysis, to average out the effects of long term variations in $\delta^{13}\text{C}$ (Seuss effect),
480 seasonal cycles, potential short-term transient stress-induced growth rate variations, effects of water use efficiency
481 (WUE), and potential short-term variations in CO₂ flux, all of which may result in time-averaged isotopic shifts over
482 different growth periods (Helle and Schleser, 2004; Verheyden et al., 2004). We include these notes as guidance in
483 Section 4.4: Lessons Learned for Future Studies. Despite the additional difficulty of conducting higher time resolution
484 analysis, this type of study holds great potential for attempting to reconstruct volcanic CO₂ histories and to study its

485 potential fertilization effect, due to the completely independent nature of the volcanic excess CO₂ supply to the sub-
486 canopy air.

487 **4.4 Lessons Learned for Future Studies**

488 This exploratory study reveals significant new potential for future studies to utilize the volcanically enhanced CO₂
489 emissions approach to study tropical ecosystem responses to eCO₂—one of the largest uncertainties in climate
490 projections. Costa Rica’s volcanoes are host to large areas of relatively undisturbed rainforest, making them ideal
491 study areas for examining responses of ecosystems to eCO₂. However, there are several challenges future studies
492 should take into consideration if attempting to expand upon this preliminary study. Given the enormous tropical
493 species diversity and the need to control for confounding factors, large datasets will be needed to answer these
494 questions conclusively. One open question for example is how WUE in upper and lower canopy leaves of same and
495 different individuals within a species may affect isotopic sequestration of CO₂. Since the excess volcanic CO₂ is
496 naturally isotopically labelled, this could be assessed by a much more detailed by-individual tree leaf, branch, and
497 xylem core study coupled with long-term measurements of evapotranspiration, heat stress, and stomatal conductance,
498 the latter of which in our study showed no significant correlation with the δ¹³C signal in the wood cores across spatial
499 gradients. Field data can be difficult to acquire in these rugged and challenging environments. A remote sensing
500 approach using airborne measurements, validated by targeted representative ground campaigns, could provide
501 sufficiently large data sets to represent species diversity and conditions appropriately. Many of the datatypes that
502 would be useful for this type of study can be acquired from airborne platforms, and remote sensing instruments can
503 quickly produce the massive datasets required to provide more comprehensive answers to these questions.

504
505 Our results also offer significant new tools for the volcanology, where reconstructing past volcano behavior through
506 eruption histories is hampered by severe preservation gaps in the stratigraphic record. A strong link between δ¹³C and
507 volcanic CO₂ could be a game-changer by establishing long-term histories of volcanic CO₂ emission variations . These
508 proxy signals could be traced back in time using living and preserved dead trees, in order to fill gaps in the historical
509 and monitoring records – a boon for volcano researchers and observatories to improve eruption prediction capabilities
510 (Newhall et al., 2017; Pyle, 2017; Sparks et al., 2012). However, this would require orders of magnitudes more
511 analyses than currently done in volcanology. While variations in tree ring ¹⁴C content have been shown to correlate
512 well with variations in volcanic CO₂ flux (Evans et al., 2010; Lefevre et al., 2017; Lewicki and Hilley, 2014), ¹³C is
513 inexpensive to measure at more laboratories, allowing for substantially more data to be acquired. Independent
514 validation, and calibration by wood core dendrochronology via ¹⁴C, tree rings, or chemical event tracers like sulfur
515 isotopes, could significantly advance the concept of using wood carbon as archives of past degassing activity.
516 Furthermore, knowledge of the short-term real-time response of leaves to diffusely emitted eCO₂, which is more likely
517 to represent deeper processes inside volcanoes than crater-area degassing (Camarda et al., 2012), may permit the use
518 of trees as sensors of transient changes in volcanic degassing indicative of volcanic reactivation and deep magma
519 movement possibly leading up to eruptions (Camarda et al., 2012; Pieri et al., 2016; Schwandner et al., 2017;
520 Shinohara et al., 2008; Werner et al., 2013).

521 **5 Conclusions**

522 Multiple areas of dense tropical forest on two Costa Rican active volcanoes are consistently and continuously exposed
523 to volcanically-elevated levels of atmospheric CO₂, diffusively cold-emitted through soils into overlying forests.
524 These isotopically heavy volcanic CO₂ emissions, which are mostly invariant, not accompanied by acidic gases, and
525 independent of processes affecting growth rates, are well correlated with increases in heavy carbon signatures in wood
526 cores from two species of tropical trees, possibly suggesting long-term incorporation of enhanced levels of
527 volcanically emitted CO₂ into biomass. Each tree studied was co-located with a soil CO₂ flux measurement and their
528 soil CO₂ flux signals vary spatially around a continuous long-term local natural excess volcanic CO₂ source, which
529 creates a local CO₂ gradient within which all the sampled trees are found. The excess volcanic CO₂ through local fault-
530 bound gas seeps provides continuous exposure to all sampled trees over time scales much greater than the lifetimes of
531 individual trees. Based on our limited exploratory measurements, confounding factors that are known to influence
532 $\delta^{13}\text{C}$ values in wood appear not to have significantly affected our measurements, indicating that the heavier wood $\delta^{13}\text{C}$
533 values could be caused by photosynthetic incorporation of volcanic excess CO₂. One of the three species studied (*A.*
534 *acuminata*) has consistent positive correlations between instantaneous plant function measurements and diffuse CO₂
535 flux measurements, indicating that short-term variations in elevated CO₂ emissions may measurably affect trees
536 growing in areas of diffuse volcanic gas emissions. These observations reveal significant potential for future studies
537 to use these areas of naturally elevated CO₂ to study ecosystem responses to elevated CO₂, and to use trees as sensors
538 of changing degassing behavior of volcanic flanks, which is indicative of deep magmatic processes.

539
540 *Data availability.* Data can be found in Table S1 and Table S2 in the supplement or can be requested from Florian
541 Schwandner (Florian.Schwandner@jpl.nasa.gov).

542
543 *Author contributions.* FMS and JBF designed the study, and RRB, FMS, JBF, and ED conducted the field work and
544 collected all samples and data with some of the equipment borrowed from GN, who helped interpret the results. TSM
545 processed the samples for analysis. JPL conducted the SO₂ analysis, wrote the related methods subsection, and helped
546 interpret the results. VY modelled the anthropogenic CO₂ emissions, wrote the related methods subsection, and helped
547 interpret the results. CAF created the combined figure showing the CO₂ and SO₂ results and assisted in writing the
548 manuscript. RRB wrote the publication, with contributions from all co-authors.

549
550 *Competing interests.* The authors declare that they have no conflict of interest.

551 **Acknowledgements**

552 We are grateful for LI-COR, Inc. (Lincoln, NE, USA) providing us a loaner CO₂ sensor for field work in Costa Rica.
553 We thank Rizalina Schwandner for engineering assistance during sensor integration, OVSICORI (Observatorio
554 Vulcanológico y Sismológico de Costa Rica, the Costa Rican volcano monitoring authority) for logistical and permit
555 support, SINAC (Sistema Nacional de Áreas de Conservación, the Costa Rican National Parks Service) for access at

556 Turrialba volcano, as well as Mr. Marco Antonio Otárola Rojas (Universidad Nacional de Costa Rica – ICOMVIS)
557 for invaluable help in the field. Incidental funding is acknowledged from the S.W. Hartman Fund at Occidental College
558 for funding R.R.B.'s field expenses, as well as the Jet Propulsion Laboratory's YIP (Year-round Internship Program)
559 and the Jet Propulsion Laboratory Education Office for funding and support for R.R.B. F.M.S.'s UCLA contribution
560 to this work was supported by Jet Propulsion Laboratory subcontract 1570200. Part of the research described in this
561 paper was carried out at the Jet Propulsion Laboratory, California Institute of Technology, under a contract with the
562 National Aeronautics and Space Administration.

563 **References**

564 Ainsworth, E. A. and Long, S. P.: What have we learned from 15 years of free-air CO₂ enrichment (FACE)? A meta-
565 analytic review of the responses of photosynthesis, canopy properties and plant production to rising CO₂, *New Phytol.*,
566 165(2), 351–372, doi:10.1111/j.1469-8137.2004.01224.x, 2005.

567 Aiuppa, A., Caleca, A., Federico, C., Gurrieri, S. and Valenza, M.: Diffuse degassing of carbon dioxide at Somma-
568 Vesuvius volcanic complex (Southern Italy) and its relation with regional tectonics, *J. Volcanol. Geotherm. Res.*,
569 133(1), 55–79, doi:10.1016/S0377-0273(03)00391-3, 2004.

570 Alvarado, G. E., Carr, M. J., Turrin, B. D., Swisher, C. C., Schmincke, H.-U. and Hudnut, K. W.: Recent volcanic
571 history of Irazú volcano, Costa Rica: Alternation and mixing of two magma batches, and pervasive mixing, in *Special*
572 *Paper 412: Volcanic Hazards in Central America*, vol. 412, pp. 259–276, Geological Society of America., 2006.

573 Baker, N. R. and Oxborough, K.: Chlorophyll Fluorescence as a Probe of Photosynthetic Productivity, in *Chlorophyll*
574 *a Fluorescence*, pp. 65–82, Springer, Dordrecht., 2004.

575 Barquero, R., Lesage, P., Metaxian, J. P., Creusot, A. and Fernández, M.: La crisis sísmica en el volcán Irazú en 1991
576 (Costa Rica), *Rev. Geológica América Cent.*, 0(18), doi:10.15517/rzac.v0i18.13494, 1995.

577 Belikov, D. A., Maksyutov, S., Yaremchuk, A., Ganshin, A., Kaminski, T., Blessing, S., Sasakawa, M., Gomez-
578 Pelaez, A. J. and Starchenko, A.: Adjoint of the global Eulerian–Lagrangian coupled atmospheric transport model (A-
579 GELCA v1.0): development and validation, *Geosci. Model Dev.*, 9(2), 749–764, doi:10.5194/gmd-9-749-2016, 2016.

580 Biondi, F. and Fessenden, J. E.: Response of lodgepole pine growth to CO₂ degassing at Mammoth Mountain,
581 California, *Ecol. Brooklyn*, 80(7), 2420–2426, 1999.

582 Burton, M. R., Sawyer, G. M. and Granieri, D.: Deep Carbon Emissions from Volcanoes, *Rev. Mineral. Geochem.*,
583 75(1), 323–354, doi:10.2138/rmg.2013.75.11, 2013.

584 Camarda, M., Gurrieri, S. and Valenza, M.: CO₂ flux measurements in volcanic areas using the dynamic concentration
585 method: Influence of soil permeability, *J. Geophys. Res. Solid Earth*, 111(B5), B05202, doi:10.1029/2005JB003898,
586 2006.

587 Camarda, M., De Gregorio, S. and Gurrieri, S.: Magma-ascent processes during 2005–2009 at Mt Etna inferred by
588 soil CO₂ emissions in peripheral areas of the volcano, *Chem. Geol.*, 330–331, 218–227,
589 doi:10.1016/j.chemgeo.2012.08.024, 2012.

590 Champion, R., Salerno, G. G., Coheur, P.-F., Hurtmans, D., Clarisse, L., Kazahaya, K., Burton, M., Caltabiano, T.,
591 Clerbaux, C. and Bernard, A.: Measuring volcanic degassing of SO₂ in the lower troposphere with ASTER band ratios,
592 *J. Volcanol. Geotherm. Res.*, 194(1–3), 42–54, doi:10.1016/j.jvolgeores.2010.04.010, 2010.

- 593 Cardellini, C., Chiodini, G. and Frondini, F.: Application of stochastic simulation to CO₂ flux from soil: Mapping and
594 quantification of gas release, *J. Geophys. Res. Solid Earth*, 108(B9), 2425, doi:10.1029/2002JB002165, 2003.
- 595 Cawse-Nicholson, K., Fisher, J. B., Famiglietti, C. A., Braverman, A., Schwandner, F. M., Lewicki, J. L., Townsend,
596 P. A., Schimel, D. S., Pavlick, R., Borman, K., Ferraz, A. A., Ye, Z., Kang, L. E., Ma, P., Bogue, R., Youmans, T.
597 and Pieri, D. C.: Ecosystem responses to elevated CO₂ using airborne remote sensing at Mammoth Mountain,
598 California, *Biogeosciences Discuss.*, 2018.
- 599 Chiodini, G., Cioni, R., Guidi, M., Raco, B. and Marini, L.: Soil CO₂ flux measurements in volcanic and geothermal
600 areas, *Appl. Geochem.*, 13(5), 543–552, doi:10.1016/S0883-2927(97)00076-0, 1998.
- 601 Cox, P., Pearson, D., Booth, B., Friedlingstein, P., Huntingford, C., Jones, C. and Luke, C.: Sensitivity of tropical
602 carbon to climate change constrained by carbon dioxide variability., 2013.
- 603 Delmelle, P. and Stix, J.: *Volcanic Gases*, edited by H. Sigurdsson, B. Houghton, H. Rymer, J. Stix, and S. McNutt,
604 *Encyclopedia Volcanoes*, 1417, 1999.
- 605 Dietrich, V. J., Fiebig, J., Chiodini, G. and Schwandner, F. M.: Fluid Geochemistry of the Hydrothermal System, in
606 *Nisyros Volcano*, edited by V. J. Dietrich, E. Lagios, and O. Bachmann, p. 339, Springer, Berlin., 2016.
- 607 Eckhardt, S., Cassiani, M., Evangeliou, N., Sollum, E., Pisso, I. and Stohl, A.: Source–receptor matrix calculation for
608 deposited mass with the Lagrangian particle dispersion model FLEXPART v10.2 in backward mode, *Geosci. Model*
609 *Dev. Katlenburg-Lindau*, 10(12), 4605–4618, doi:http://dx.doi.org/10.5194/gmd-10-4605-2017, 2017.
- 610 Epiard, M., Avard, G., de Moor, J. M., Martínez Cruz, M., Barrantes Castillo, G. and Bakkar, H.: Relationship between
611 Diffuse CO₂ Degassing and Volcanic Activity. Case Study of the Poás, Irazú, and Turrialba Volcanoes, Costa Rica,
612 *Front. Earth Sci.*, 5, doi:10.3389/feart.2017.00071, 2017.
- 613 Evans, W. C., Bergfeld, D., McGeehin, J. P., King, J. C. and Heasler, H.: Tree-ring ¹⁴C links seismic swarm to CO₂
614 spike at Yellowstone, USA, *Geology*, 38(12), 1075–1078, 2010.
- 615 Farrar, C. D., Sorey, M. L., Evans, W. C., Howle, J. F., Kerr, B. D., Kennedy, B. M., King, C.-Y. and Southon, J. R.:
616 Forest-killing diffuse CO₂ emission at Mammoth Mountain as a sign of magmatic unrest, *Nature*, 376(6542), 675–
617 678, doi:10.1038/376675a0, 1995.
- 618 Friedlingstein, P., Meinshausen, M., Arora, V. K., Jones, C. D., Anav, A., Liddicoat, S. K. and Knutti, R.:
619 Uncertainties in CMIP5 Climate Projections due to Carbon Cycle Feedbacks, *J. Clim.*, 27(2), 511–526,
620 doi:10.1175/JCLI-D-12-00579.1, 2013.
- 621 Garten, C. T., Iversen, C. M. and Norby, R. J.: Litterfall ¹⁵N abundance indicates declining soil nitrogen availability
622 in a free-air CO₂ enrichment experiment, *Ecology*, 92(1), 133–139, doi:10.1890/10-0293.1, 2011.
- 623 Global Volcanism Program: *Volcanoes of the World*, v. 4.6.5, edited by E. Venzke, Smithsonian Inst.,
624 doi:https://dx.doi.org/10.5479/si.GVP.VOTW4-2013, 2013.
- 625 Gregory, J. M., Jones, C. D., Cadule, P. and Friedlingstein, P.: Quantifying Carbon Cycle Feedbacks, *J. Clim.*, 22(19),
626 5232–5250, doi:10.1175/2009JCLI2949.1, 2009.
- 627 Hebeisen, T., Lüscher, A., Zanetti, S., Fischer, B., Hartwig, U., Frehner, M., Hendrey, G., Blum, H. and Nösberger*,
628 J.: Growth response of *Trifolium repens* L. and *Lolium perenne* L. as monocultures and bi-species mixture to free air
629 CO₂ enrichment and management, *Glob. Change Biol.*, 3(2), 149–160, doi:10.1046/j.1365-2486.1997.00073.x, 1997.
- 630 Helle, G. and Schleser, G. H.: Beyond CO₂-fixation by Rubisco – an interpretation of ¹³C/¹²C variations in tree rings
631 from novel intra-seasonal studies on broad-leaf trees, *Plant Cell Environ.*, 27(3), 367–380, doi:10.1111/j.0016-
632 8025.2003.01159.x, 2004.

- 633 Kappelle, M., Geuze, T., Leal, M. E. and Cleef, A. M.: Successional age and forest structure in a Costa Rican upper
634 montane *Quercus* forest, *J. Trop. Ecol.*, 12(05), 681–698, doi:10.1017/S0266467400009871, 1996.
- 635 Kauwe, M. G. D., Keenan, T. F., Medlyn, B. E., Prentice, I. C. and Terrer, C.: Satellite based estimates underestimate
636 the effect of CO₂ fertilization on net primary productivity, *Nat. Clim. Change*, 6(10), 892, doi:10.1038/nclimate3105,
637 2016.
- 638 Keeling, C. D.: The Carbon Dioxide Cycle: Reservoir Models to Depict the Exchange of Atmospheric Carbon Dioxide
639 with the Oceans and Land Plants, in *Chemistry of the Lower Atmosphere*, edited by S. I. Rasool, pp. 251–329, Springer
640 US, Boston, MA., 1973.
- 641 Lefevre, J.-C., Gillot, P.-Y., Cardellini, C., Gresse, M., Lesage, L., Chiodini, G. and Oberlin, C.: Use of the
642 Radiocarbon Activity Deficit in Vegetation as a Sensor of CO₂ Soil Degassing: Example from La Solfatara (Naples,
643 Southern Italy), *Radiocarbon*, 1–12, doi:10.1017/RDC.2017.76, 2017.
- 644 Leigh, E. G., Losos, E. C. and Research, N. B. of E.: *Tropical forest diversity and dynamism : findings from a large-
645 scale network*, Chicago, Ill.; London: The University of Chicago Press. [online] Available from:
646 <http://trove.nla.gov.au/version/12851528> (Accessed 25 September 2017), 2004.
- 647 Lewicki, J. L. and Hilley, G. E.: Multi-scale observations of the variability of magmatic CO₂ emissions, Mammoth
648 Mountain, CA, USA, *J. Volcanol. Geotherm. Res.*, 284(Supplement C), 1–15, doi:10.1016/j.jvolgeores.2014.07.011,
649 2014.
- 650 Lewicki, J. L., Hilley, G. E., Shelly, D. R., King, J. C., McGeehin, J. P., Mangan, M. and Evans, W. C.: Crustal
651 migration of CO₂-rich magmatic fluids recorded by tree-ring radiocarbon and seismicity at Mammoth Mountain, CA,
652 USA, *Earth Planet. Sci. Lett.*, 390, 52–58, doi:10.1016/j.epsl.2013.12.035, 2014.
- 653 Lüscher, A., Hartwig, U. A., Suter, D. and Nösberger, J.: Direct evidence that symbiotic N₂ fixation in fertile grassland
654 is an important trait for a strong response of plants to elevated atmospheric CO₂, *Glob. Change Biol.*, 6(6), 655–662,
655 doi:10.1046/j.1365-2486.2000.00345.x, 2000.
- 656 Malowany, K. S., Stix, J., de Moor, J. M., Chu, K., Lacrampe-Couloume, G. and Sherwood Lollar, B.: Carbon isotope
657 systematics of Turrialba volcano, Costa Rica, using a portable cavity ring-down spectrometer, *Geochem. Geophys.
658 Geosystems*, 18(7), 2769–2784, doi:10.1002/2017GC006856, 2017.
- 659 Martini, F., Tassi, F., Vaselli, O., Del Potro, R., Martinez, M., del Laat, R. V. and Fernandez, E.: Geophysical,
660 geochemical and geodetical signals of reawakening at Turrialba volcano (Costa Rica) after almost 150 years of
661 quiescence, *J. Volcanol. Geotherm. Res.*, 198(3–4), 416–432, doi:10.1016/j.jvolgeores.2010.09.021, 2010.
- 662 Mason, E., Edmonds, M. and Turchyn, A. V.: Remobilization of crustal carbon may dominate volcanic arc emissions,
663 *Science*, 357(6348), 290–294, 2017.
- 664 McGee, K. A. and Gerlach, T. M.: Annual cycle of magmatic CO₂ in a tree-kill soil at Mammoth Mountain, California:
665 Implications for soil acidification, *Geology*, 26(5), 463–466, 1998.
- 666 de Moor, J. M., Aiuppa, A., Avaré, G., Wehrmann, H., Dunbar, N., Müller, C., Tamburello, G., Giudice, G., Liuzzo,
667 M., Moretti, R., Conde, V. and Galle, B.: Turmoil at Turrialba Volcano (Costa Rica): Degassing and eruptive processes
668 inferred from high-frequency gas monitoring, *J. Geophys. Res. Solid Earth*, 121(8), 2016JB013150,
669 doi:10.1002/2016JB013150, 2016.
- 670 Newhall, C. G., Costa, F., Ratdomopurbo, A., Venezky, D. Y., Widiwijayanti, C., Win, N. T. Z., Tan, K. and Fajiculay,
671 E.: WOVodat – An online, growing library of worldwide volcanic unrest, *J. Volcanol. Geotherm. Res.*, 345, 184–
672 199, doi:10.1016/j.jvolgeores.2017.08.003, 2017.
- 673 Nicholson, E.: *Volcanology: An Introduction*, Larsen and Keller Education., 2017.

- 674 Norby, R. J., Warren, J. M., Iversen, C. M., Medlyn, B. E. and McMurtrie, R. E.: CO₂ enhancement of forest
675 productivity constrained by limited nitrogen availability, *Proc. Natl. Acad. Sci.*, 107(45), 19368–19373,
676 doi:10.1073/pnas.1006463107, 2010.
- 677 Norby, R. J., De Kauwe, M. G., Domingues, T. F., Duursma, R. A., Ellsworth, D. S., Goll, D. S., Lapola, D. M., Luus,
678 K. A., MacKenzie, A. R., Medlyn, B. E., Pavlick, R., Rammig, A., Smith, B., Thomas, R., Thonicke, K., Walker, A.
679 P., Yang, X. and Zaehle, S.: Model–data synthesis for the next generation of forest free-air CO₂ enrichment (FACE)
680 experiments, *New Phytol.*, 209(1), 17–28, doi:10.1111/nph.13593, 2016.
- 681 Norman, E. M.: *Buddlejaceae (Flora Neotropica Monograph No. 81)*, The New York Botanical Garden Press., 2000.
- 682 Oda, T. and Maksyutov, S.: A very high-resolution (1 km×1 km) global fossil fuel CO₂ emission inventory derived
683 using a point source database and satellite observations of nighttime lights, *Atmos Chem Phys*, 11(2), 543–556,
684 doi:10.5194/acp-11-543-2011, 2011.
- 685 Ortega-Pieck, A., López-Barrera, F., Ramírez-Marcial, N. and García-Franco, J. G.: Early seedling establishment of
686 two tropical montane cloud forest tree species: The role of native and exotic grasses, *For. Ecol. Manag.*, 261(7), 1336–
687 1343, doi:10.1016/j.foreco.2011.01.013, 2011.
- 688 Paoletti, E., Seufert, G., Della Rocca, G. and Thomsen, H.: Photosynthetic responses to elevated CO₂ and O₃ in
689 *Quercus ilex* leaves at a natural CO₂ spring, *Environ. Pollut.*, 147(3), 516–524, doi:10.1016/j.envpol.2006.08.039,
690 2007.
- 691 Parry, C., Blonquist, J. M. and Bugbee, B.: In situ measurement of leaf chlorophyll concentration: analysis of the
692 optical/absolute relationship, *Plant Cell Environ.*, 37(11), 2508–2520, doi:10.1111/pce.12324, 2014.
- 693 Peiffer, L., Wanner, C. and Lewicki, J. L.: Unraveling the dynamics of magmatic CO₂ degassing at Mammoth
694 Mountain, California, *Earth Planet. Sci. Lett.*, 484, 318–328, doi:10.1016/j.epsl.2017.12.038, 2018.
- 695 Pérez, N., Hernandez, P., Padilla, G., Nolasco, D., Barrancos, J., Melián, G., Padrón, E., Dionis, S., Calvo, D. and
696 Rodríguez, F.: Global CO₂ emission from volcanic lakes., 2011.
- 697 Pieri, D., Schwandner, F. M., Realmuto, V. J., Lundgren, P. R., Hook, S., Anderson, K., Buongiorno, M. F., Diaz, J.
698 A., Gillespie, A., Miklius, A., Mothes, P., Mougins-Mark, P., Pallister, M., Poland, M., Palgar, L. L., Pata, F.,
699 Pritchard, M., Self, S., Sigmundsson, F., de Silva, S. and Webley, P.: Enabling a global perspective for deterministic
700 modeling of volcanic unrest, [online] Available from:
701 https://hyspirci.jpl.nasa.gov/downloads/RFI2_HyspIRI_related_160517/RFI2_final_PieriDavidC-final-rev.pdf
702 (Accessed 20 February 2018), 2016.
- 703 Pinkard, E. A., Beadle, C. L., Mendham, D. S., Carter, J. and Glen, M.: Determining photosynthetic responses of
704 forest species to elevated CO₂: alternatives to FACE, *For. Ecol. Manag.*, 260(8), 1251–1261, 2010.
- 705 Pyle, D. M.: What Can We Learn from Records of Past Eruptions to Better Prepare for the Future?, in SpringerLink,
706 pp. 1–18, Springer, Berlin, Heidelberg., 2017.
- 707 Quintana-Ascencio, P. F., Ramírez-Marcial, N., González-Espinosa, M. and Martínez-Icó, M.: Sapling survival and
708 growth of coniferous and broad-leaved trees in successional highland habitats in Mexico, *Appl. Veg. Sci.*, 7(1), 81–
709 88, 2004.
- 710 Rizzo, A. L., Di Piazza, A., de Moor, J. M., Alvarado, G. E., Avaró, G., Carapezza, M. L. and Mora, M. M.: Eruptive
711 activity at Turrialba volcano (Costa Rica): Inferences from ³He/⁴He in fumarole gases and chemistry of the products
712 ejected during 2014 and 2015: ERUPTIVE ACTIVITY AT TURRIALBA VOLCANO, *Geochem. Geophys.*
713 *Geosystems*, 17(11), 4478–4494, doi:10.1002/2016GC006525, 2016.

- 714 Saha, S., Moorthi, S., Pan, H.-L., Wu, X., Wang, J., Nadiga, S., Tripp, P., Kistler, R., Woollen, J., Behringer, D., Liu,
715 H., Stokes, D., Grumbine, R., Gayno, G., Wang, J., Hou, Y.-T., Chuang, H., Juang, H.-M. H., Sela, J., Iredell, M.,
716 Treadon, R., Kleist, D., Van Delst, P., Keyser, D., Derber, J., Ek, M., Meng, J., Wei, H., Yang, R., Lord, S., van den
717 Dool, H., Kumar, A., Wang, W., Long, C., Chelliah, M., Xue, Y., Huang, B., Schemm, J.-K., Ebisuzaki, W., Lin, R.,
718 Xie, P., Chen, M., Zhou, S., Higgins, W., Zou, C.-Z., Liu, Q., Chen, Y., Han, Y., Cucurull, L., Reynolds, R. W.,
719 Rutledge, G. and Goldberg, M.: NCEP Climate Forecast System Reanalysis (CFSR) 6-hourly Products, January 1979
720 to December 2010, *Bull. Am. Meteorol. Soc.*, 91(8), 1015–1058, doi:10.5065/D69K487J, 2010a.
- 721 Saha, S., Moorthi, S., Pan, H.-L., Wu, X., Wang, J., Nadiga, S., Tripp, P., Kistler, R., Woollen, J., Behringer, D., Liu,
722 H., Stokes, D., Grumbine, R., Gayno, G., Wang, J., Hou, Y.-T., Chuang, H., Juang, H.-M. H., Sela, J., Iredell, M.,
723 Treadon, R., Kleist, D., Van Delst, P., Keyser, D., Derber, J., Ek, M., Meng, J., Wei, H., Yang, R., Lord, S., van den
724 Dool, H., Kumar, A., Wang, W., Long, C., Chelliah, M., Xue, Y., Huang, B., Schemm, J.-K., Ebisuzaki, W., Lin, R.,
725 Xie, P., Chen, M., Zhou, S., Higgins, W., Zou, C.-Z., Liu, Q., Chen, Y., Han, Y., Cucurull, L., Reynolds, R. W.,
726 Rutledge, G. and Goldberg, M.: The NCEP Climate Forecast System Reanalysis, *Bull. Am. Meteorol. Soc.*, 91(8),
727 1015–1058, doi:10.1175/2010BAMS3001.1, 2010b.
- 728 Saurer, M., Cherubini, P., Bonani, G. and Siegwolf, R.: Tracing carbon uptake from a natural CO₂ spring into tree
729 rings: an isotope approach, *Tree Physiol.*, 23(14), 997–1004, doi:10.1093/treephys/23.14.997, 2003.
- 730 Schimel, D., Stephens, B. B. and Fisher, J. B.: Effect of increasing CO₂ on the terrestrial carbon cycle, *Proc. Natl.*
731 *Acad. Sci.*, 112(2), 436–441, doi:10.1073/pnas.1407302112, 2015.
- 732 Schwandner, F. M., Seward, T. M., Gize, A. P., Hall, P. A. and Dietrich, V. J.: Diffuse emission of organic trace gases
733 from the flank and crater of a quiescent active volcano (Vulcano, Aeolian Islands, Italy), *J. Geophys. Res.*
734 *Atmospheres*, 109(D4), D04301, doi:10.1029/2003JD003890, 2004.
- 735 Schwandner, F. M., Gunson, M. R., Miller, C. E., Carn, S. A., Eldering, A., Krings, T., Verhulst, K. R., Schimel, D.
736 S., Nguyen, H. M., Crisp, D., O'Dell, C. W., Osterman, G. B., Iraci, L. T. and Podolske, J. R.: Spaceborne detection
737 of localized carbon dioxide sources, *Science*, 358(6360), eaam5782, doi:10.1126/science.aam5782, 2017.
- 738 Sharma, S. and Williams, D.: Carbon and oxygen isotope analysis of leaf biomass reveals contrasting photosynthetic
739 responses to elevated CO₂ near geologic vents in Yellowstone National Park, *Biogeosciences*, 6(1), 25,
740 doi:10.5194/bg-6-25-2009, 2009.
- 741 Shinohara, H., Aiuppa, A., Giudice, G., Gurrieri, S. and Liuzzo, M.: Variation of H₂O/CO₂ and CO₂/SO₂ ratios of
742 volcanic gases discharged by continuous degassing of Mount Etna volcano, Italy, *J. Geophys. Res. Solid Earth*,
743 113(B9), doi:10.1029/2007JB005185, 2008.
- 744 Sinclair, A. J.: Selection of threshold values in geochemical data using probability graphs, *J. Geochem. Explor.*, 3(2),
745 129–149, doi:10.1016/0375-6742(74)90030-2, 1974.
- 746 Sorey, M. L., Evans, W. C., Kennedy, B. M., Farrar, C. D., Hainsworth, L. J. and Hausback, B.: Carbon dioxide and
747 helium emissions from a reservoir of magmatic gas beneath Mammoth Mountain, California, *J. Geophys. Res. Solid*
748 *Earth*, 103(B7), 15303–15323, doi:10.1029/98JB01389, 1998.
- 749 Sparks, R. S. J., Biggs, J. and Neuberg, J. W.: Monitoring Volcanoes, *Science*, 335(6074), 1310–1311,
750 doi:10.1126/science.1219485, 2012.
- 751 Staebler, R. M. and Fitzjarrald, D. R.: Observing subcanopy CO₂ advection, *Agric. For. Meteorol.*, 122(3–4), 139–
752 156, doi:10.1016/j.agrformet.2003.09.011, 2004.
- 753 Stine, C. M. and Banks, N. G.: Costa Rica Volcano Profile, USGS Numbered Series, U.S. Geological Survey. [online]
754 Available from: <https://pubs.er.usgs.gov/publication/ofr91591>, 1991.

- 755 Stohl, A. and Thomson, D. J.: A Density Correction for Lagrangian Particle Dispersion Models, *Bound.-Layer Meteorol.*, 90(1), 155–167, doi:10.1023/A:1001741110696, 1999.
- 756
- 757 Stohl, A., Hittenberger, M. and Wotawa, G.: Validation of the Lagrangian particle dispersion model FLEXPART against large-scale tracer experiment data, *Atmos. Environ.*, 32(24), 4245–4264, 1998.
- 758
- 759 Stohl, A., Forster, C., Frank, A., Seibert, P. and Wotawa, G.: Technical note: The Lagrangian particle dispersion model FLEXPART version 6.2, *Atmospheric Chem. Phys.*, 5(9), 2461–2474, doi:https://doi.org/10.5194/acp-5-2461-2005, 2005.
- 760
- 761
- 762 Symonds, R. B., Gerlach, T. M. and Reed, M. H.: Magmatic gas scrubbing: implications for volcano monitoring, *J. Volcanol. Geotherm. Res.*, 108(1), 303–341, doi:10.1016/S0377-0273(00)00292-4, 2001.
- 763
- 764 Tanner, E. V. J., Vitousek, P. M. and Cuevas, E.: Experimental Investigation of Nutrient Limitation of Forest Growth on Wet Tropical Mountains, *Ecology*, 79(1), 10–22, doi:10.1890/0012-9658(1998)079[0010:EIONLO]2.0.CO;2, 1998.
- 765
- 766
- 767 Tercek, M. T., Al-Niemi, T. S. and Stout, R. G.: Plants Exposed to High Levels of Carbon Dioxide in Yellowstone National Park: A Glimpse into the Future?, *Yellowstone Sci.*, 16(1), 12–19, 2008.
- 768
- 769 Thomas, C. K.: Variability of Sub-Canopy Flow, Temperature, and Horizontal Advection in Moderately Complex Terrain, *Bound.-Layer Meteorol.*, 139(1), 61–81, doi:10.1007/s10546-010-9578-9, 2011.
- 770
- 771 Townsend, A. R., Cleveland, C. C., Houlton, B. Z., Alden, C. B. and White, J. W.: Multi-element regulation of the tropical forest carbon cycle, *Front. Ecol. Environ.*, 9(1), 9–17, doi:10.1890/100047, 2011.
- 772
- 773 Verheyden, A., Helle, G., Schleser, G. H., Dehairs, F., Beeckman, H. and Koedam, N.: Annual cyclicality in high-resolution stable carbon and oxygen isotope ratios in the wood of the mangrove tree *Rhizophora mucronata*, *Plant Cell Environ.*, 27(12), 1525–1536, doi:10.1111/j.1365-3040.2004.01258.x, 2004.
- 774
- 775
- 776 Viveiros, F., Ferreira, T., Silva, C. and Gaspar, J.: Meteorological factors controlling soil gases and indoor CO₂ concentration: A permanent risk in degassing areas, *Sci. Total Environ.*, 407(4), 1362–1372, doi:10.1016/j.scitotenv.2008.10.009, 2009.
- 777
- 778
- 779 Vodnik, D., Thomalla, A., Ferlan, M., Levanič, T., Eler, K., Ogrinc, N., Wittmann, C. and Pfanz, H.: Atmospheric and geogenic CO₂ within the crown and root of spruce (*Picea abies* L. Karst.) growing in a mofette area, *Atmos. Environ.*, 182, 286–295, doi:10.1016/j.atmosenv.2018.03.043, 2018.
- 780
- 781
- 782 Weng, C., Bush, M. B. and Chepstow-Lusty, A. J.: Holocene changes of Andean alder (*Alnus acuminata*) in highland Ecuador and Peru, *J. Quat. Sci.*, 19(7), 685–691, doi:10.1002/jqs.882, 2004.
- 783
- 784 Werner, C., Kelly, P. J., Doukas, M., Lopez, T., Pfeffer, M., McGimsey, R. and Neal, C.: Degassing of CO₂, SO₂, and H₂S associated with the 2009 eruption of Redoubt Volcano, Alaska, *J. Volcanol. Geotherm. Res.*, 259, 270–284, doi:10.1016/j.jvolgeores.2012.04.012, 2013.
- 785
- 786
- 787 Werner, C., Bergfeld, D., Farrar, C. D., Doukas, M. P., Kelly, P. J. and Kern, C.: Decadal-scale variability of diffuse CO₂ emissions and seismicity revealed from long-term monitoring (1995–2013) at Mammoth Mountain, California, USA, *J. Volcanol. Geotherm. Res.*, 289, 51–63, doi:10.1016/j.jvolgeores.2014.10.020, 2014.
- 788
- 789
- 790 Williams-Jones, G., Stix, J., Heiligmann, M., Charland, A., Lollar, B. S., Arner, N., Garzón, G. V., Barquero, J. and Fernandez, E.: A model of diffuse degassing at three subduction-related volcanoes, *Bull. Volcanol.*, 62(2), 130–142, 2000.
- 791
- 792
- 793
- 794

795
796

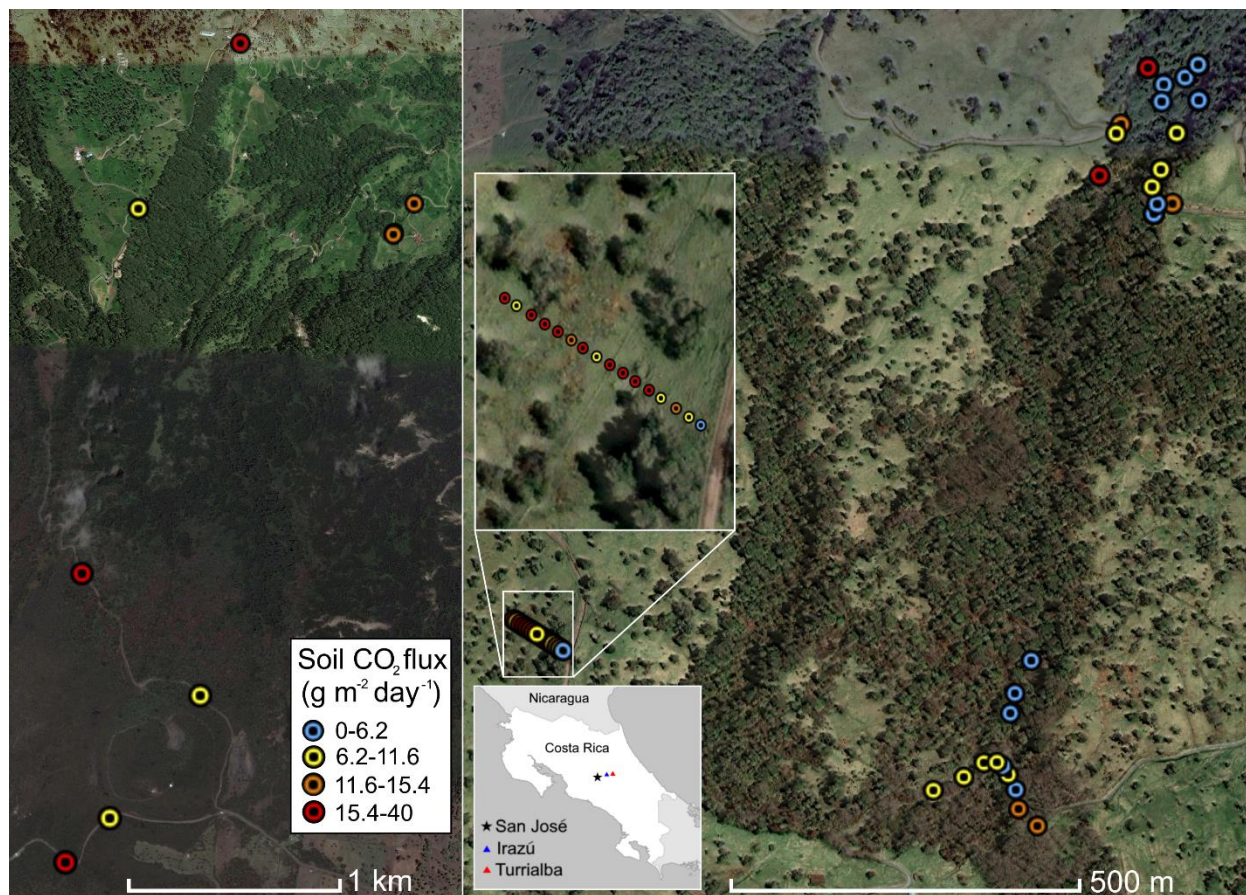
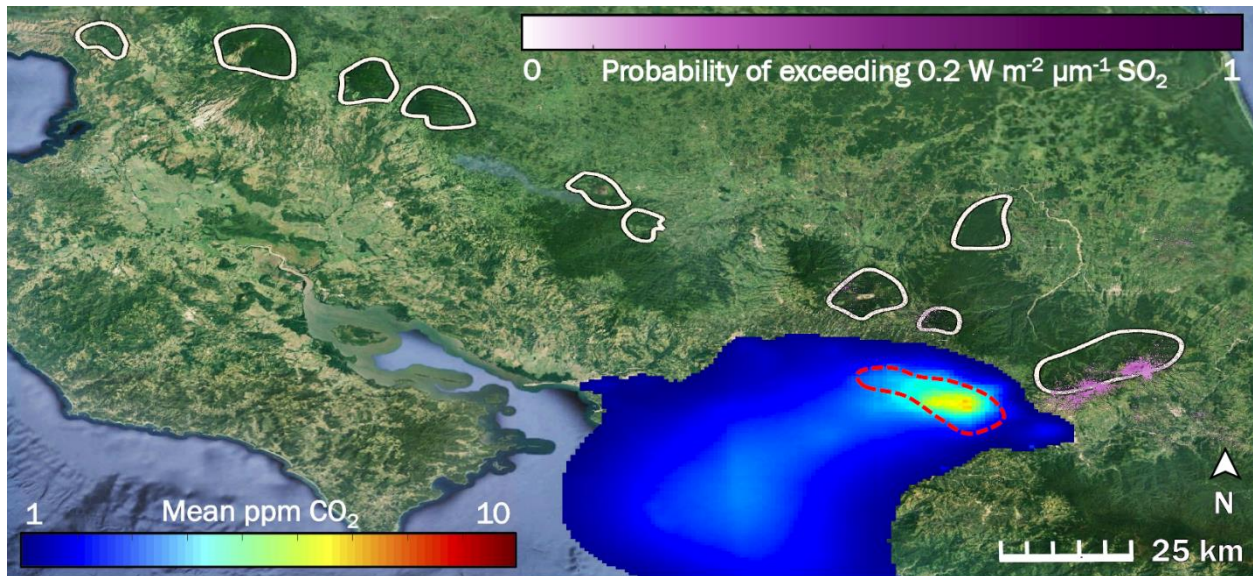


Fig. 1: Overview of measurement locations in two old-growth forests on the upper flanks of two active volcanoes in Costa Rica, Turrialba and Irazú. Distribution of mean soil CO₂ flux across north flank of Irazú (left) and south flank of Turrialba (right). Colors of dots correspond to flux populations (see Fig. 3).



797

Fig. 2: The influence of two potentially confounding gases on our study area (right hand white polygon) in Costa Rica is low to non-existent: anthropogenic CO₂ from San José (blue to red color scale), and volcanic SO₂ (purple color scale). White polygons are drawn around locations of the forested active volcanic edifices in Costa Rica. The dashed red line indicates the rough border of the San José urban area. Prevailing winds throughout the year consistently blow all anthropogenic CO₂ away from our study area and from all other white polygons.

798
799
800

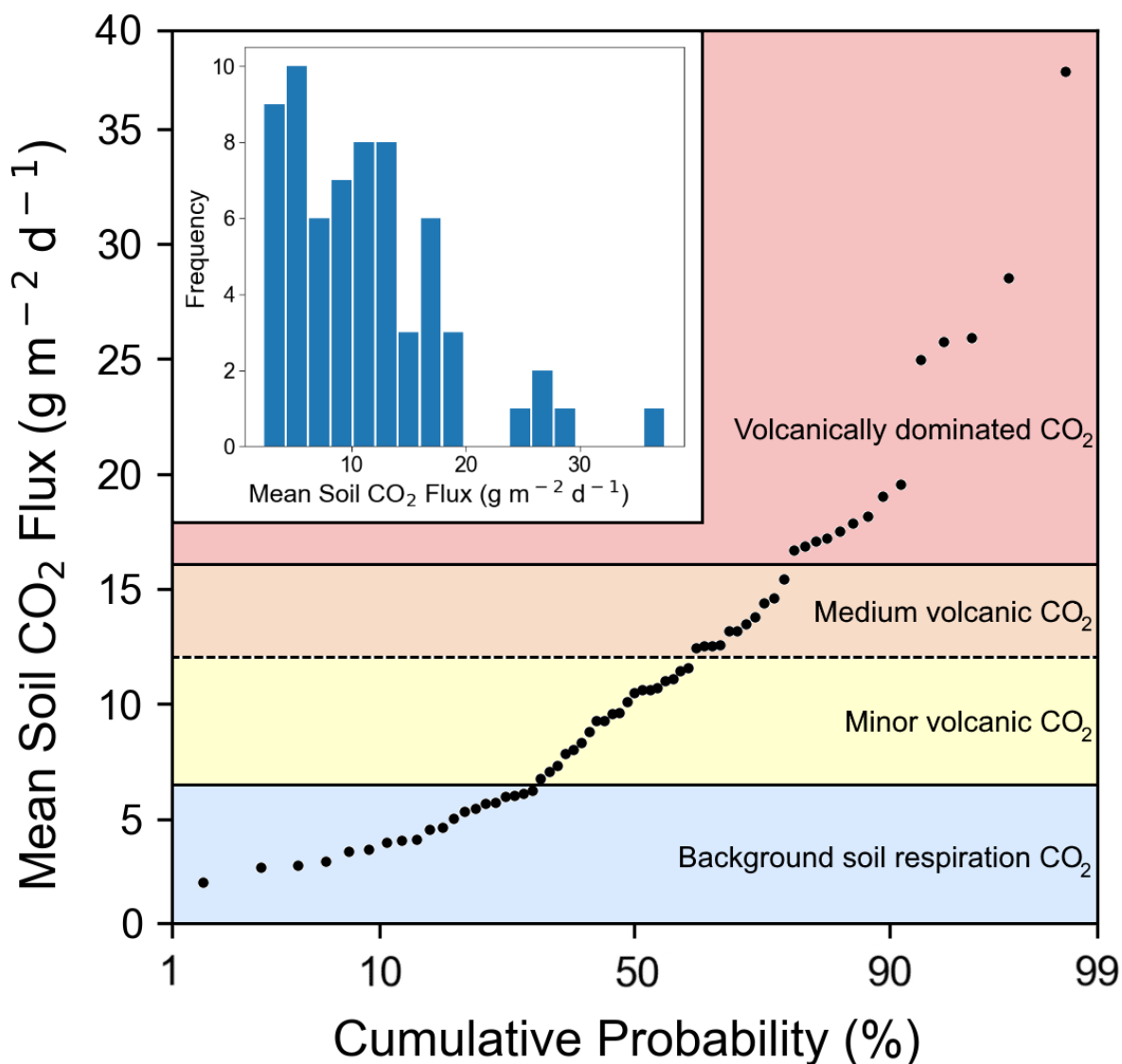


Fig 3: Soil CO₂ flux into the sub-canopy air of forests on the Turrialba-Irazú volcanic complex is pervasively and significantly influenced by a deep volcanic gas source. At least four different overlapping populations of soil CO₂ flux were identified, using a cumulative probability plot, where inflection points indicate population boundaries (Sinclair 1974). 69% of sampling locations (45 total) are exposed to varying degrees of volcanically derived elevated CO₂. Populations are color-coded based on the same color scale as Fig. 1.

801
802
803

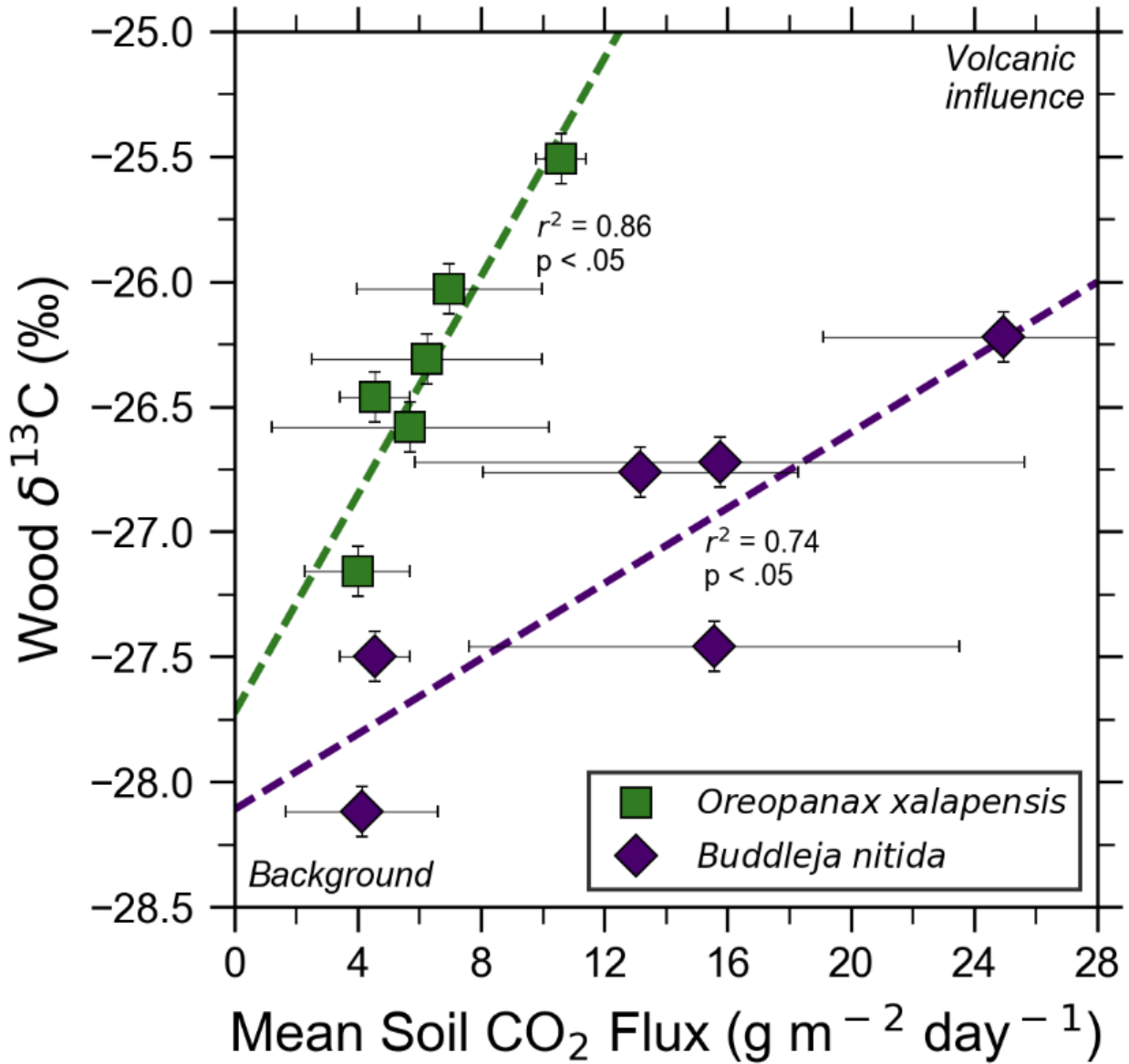


Fig 4: Bulk wood $\delta^{13}\text{C}$ of trees on Costa Rica's Turrialba volcano shows strong correlations with increasing volcanic CO_2 flux for two species, *O. xalapensis* and *B. nitida*, indicating long-term photosynthetic incorporation of isotopically heavy volcanic CO_2 . Stable carbon isotope ratio ($\delta^{13}\text{C}$) of wood cores are plotted against soil CO_2 flux measured immediately adjacent to the tree that the core sample was taken from. Background and volcanic influence labels apply to both axes – higher CO_2 flux and heavier (less negative) $\delta^{13}\text{C}$ values are both characteristic of volcanic CO_2 emissions.

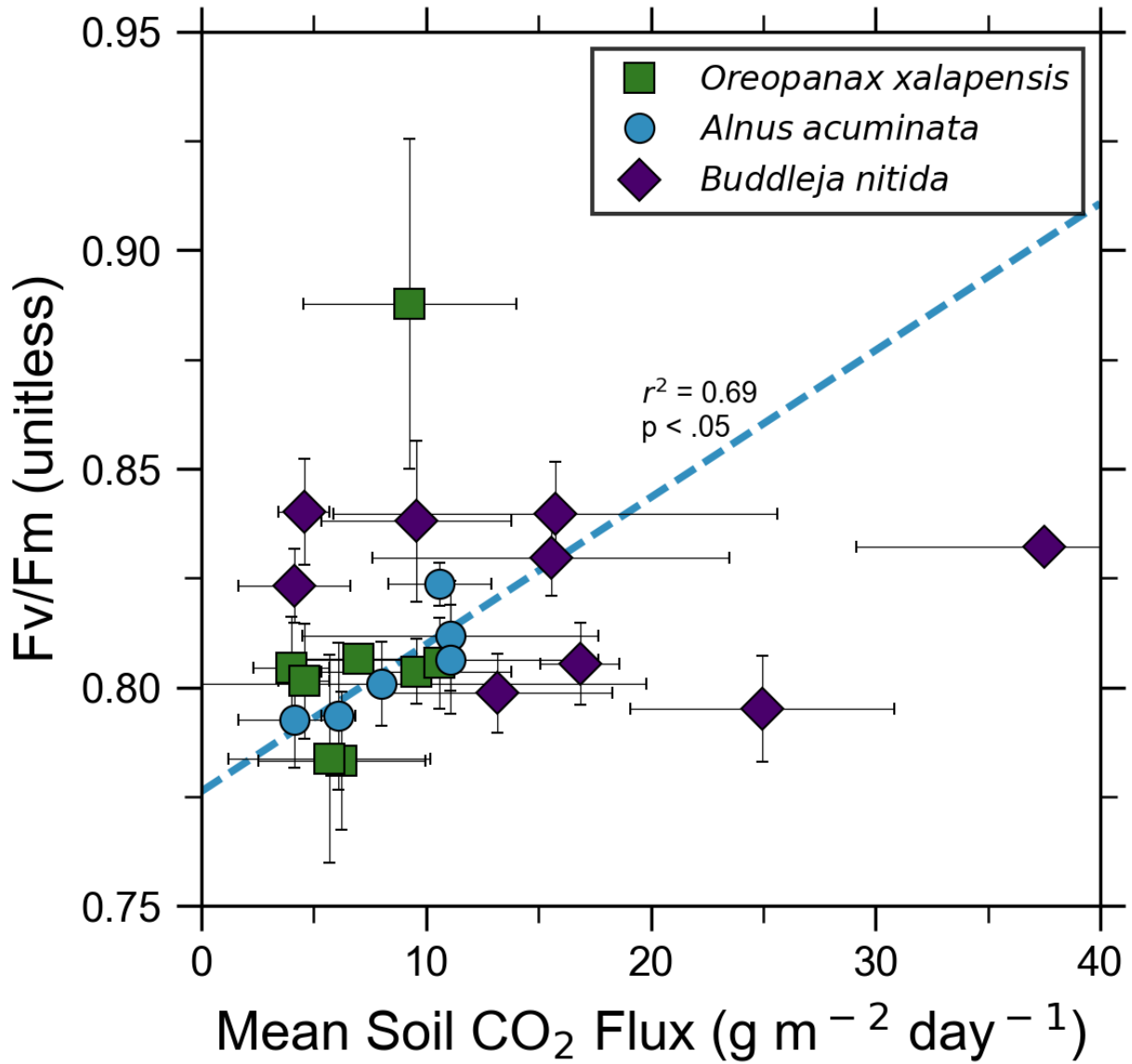
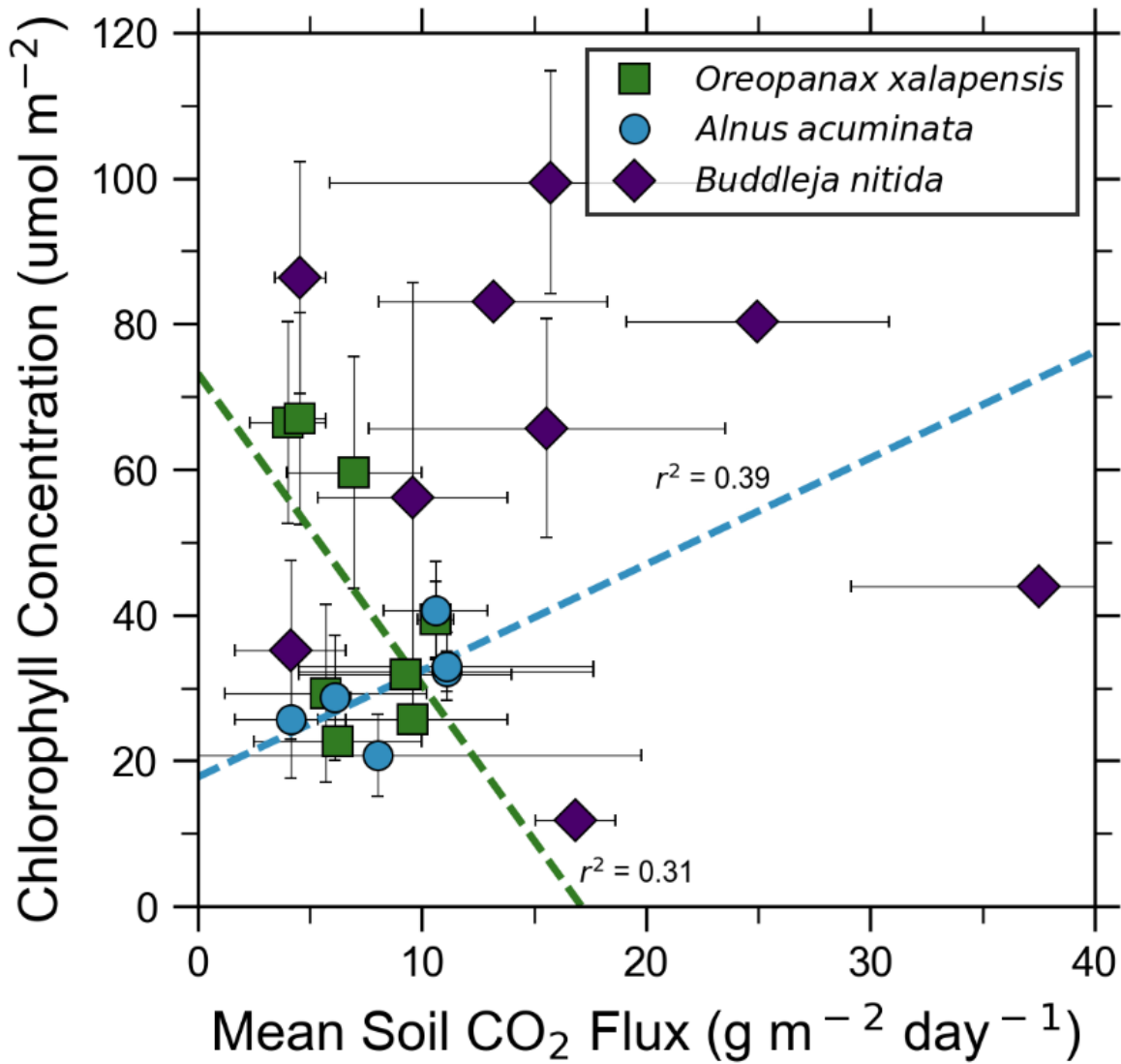


Fig. 5: Photosynthetic activity of some tree species in old-growth forests on the upper flanks of two active volcanoes in Costa Rica, Turrialba and Irazú, may show short-term response to volcanically elevated CO₂. Leaf fluorescence (Fv/Fm) and soil CO₂ flux were strongly correlated for *A. acuminata*, but not for other species.

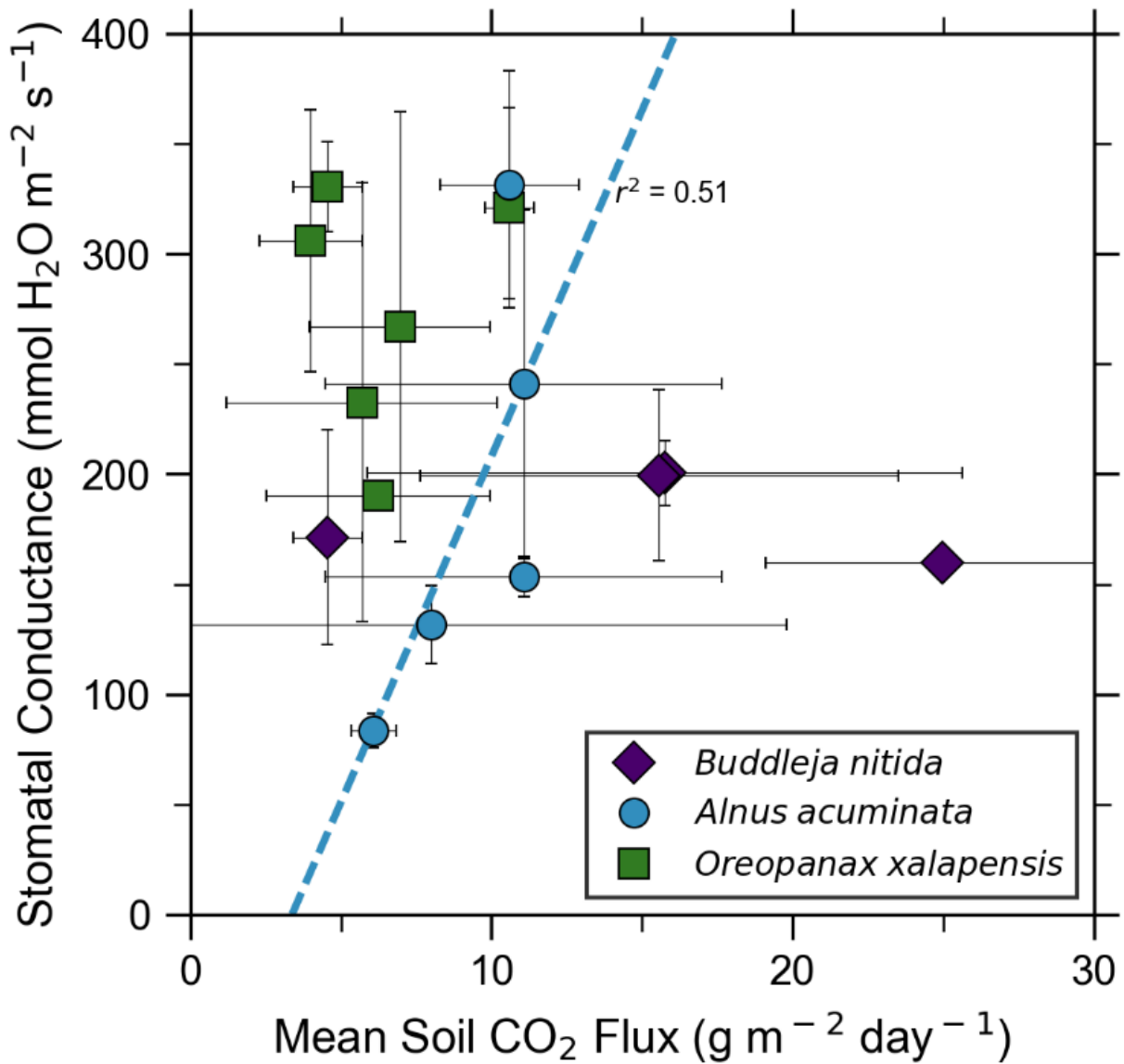


805

Fig. 6: Some tree species in old-growth forests on the upper flanks of two active volcanoes in Costa Rica, Turrialba and Irazú, may express their short-term response to volcanically elevated CO₂ by producing more chlorophyll. A species that showed strong short-term response (*A. Acuminata*, Fig. 5) also shows a positive correlation between chlorophyll concentration and mean soil CO₂ flux.

806

807



808

Fig. 7: Leaf stomatal conductance of a tree species that strongly responds to volcanically elevated CO₂ (Figs. 5, 6) has positive correlations with volcanic CO₂ flux, consistent with increased gas-exchange.

809